Supplementary Information (SI) for ChemComm.

Supporting Information

Monomer-Level Strategy for High Refractive Index without Visible-Light Absorption: Vinylthiophene Incorporation into Group 14 scaffolds

Kanon Hirota, Yuta Takemasa, Tomoki Nakagawa and Jun Terao

Department of Basic Science, Graduate School of Arts and Sciences, The University of Tokyo, 3-8-1 Komaba, Meguro-ku, Tokyo 153-8902, Japan

E-mail: ctakemasa@g.ecc.u-tokyo.ac.jp, cterao@mail.ecc.u-tokyo.ac.jp

List of Contents

S8. References

S1. General Information

S1.1. Instrumentation

^{1}H NMR (500 MHz), ^{13}C{^{1}H} NMR (126 MHz), ^{29}Si{^{1}H} NMR (99 MHz) spectra were measured with a Bruker AVANCE III HD 500. The ^{1}H NMR chemical shifts were reported relative to residual protonated solvents in DMSO-d_6 (2.50 ppm). The ^{13}C{^{1}H} NMR chemical shifts were reported relative to DMSO-d_6 (39.52 ppm). The ^{29}Si{^{1}H} NMR chemical shifts were reported by using TMS (0.00 ppm) as an external standard. Atmospheric pressure chemical ionization time-of-flight (APCI-TOF) mass spectra were recorded in positive mode on a Bruker micrOTOF II-KE02. CH_3CN was used as solvent for APCI-TOF mass spectrum measurements. The HR-MS spectra were internally calibrated using PEG or NaTFA clusters. Absorption spectra were measured with a UV-vis absorption spectrometer (Shimadzu, UV-2600). In optical analyses, solution samples were prepared in CH_3CN for measuring their absorbance and solid-state absorption spectra were measured by a diffuse reflectance method using with $BaSO_4$ as the reference. The refractive indices of the monomers prior to curing, was measured using the Atago (Tokyo, Japan) NAR-4T digital abbe refractometer. The refractive index after curing was determined by a spectroscopic ellipsometer, Horiba AUTO SE. Fourier-transform infrared (IR) spectra were recorded by JASCO FT /IR-4100 with the attenuated total reflection (ATR) method (attached kid: JASCO ATR PRO450-S).

S1.2. Materials

All regents were commercially obtained and used as received unless otherwise noted. Degassed tetrahydrofuran (THF) was purchased from Kanto Chemical and further purified by passage through active alumina under positive nitrogen pressure as described by Grubbs *et al.*[1] Methanol (CH_3OH), ethyl acetate (EtOAc), acetone, acetonitrile (CH_3CN), 5-bromothiophene-2-carboxaldehyde and *n*-butyllithium, in hexane, 1.6 mol/L were purchased from Kanto Chemical Co., Inc. Chloroform ($CHCl_3$), potassium tert-butoxide, germanium(IV) chloride and 2,2,6,6-tetramethylpiperidine 1-oxyl free radical (TEMPO) were purchased from FUJIFILM Wako Chemical Corporation. Methyltriphenylphosphonium bromide, tetrachlorosilane, chlorotriethylsilane, dimethyldichlorosilane, trichloro(methyl)silane and 1,2-ethanedithiol were purchased from Tokyo Chemical Industry (TCI) Co., Ltd. Tin(IV) chloride were purchased from Sigma-Aldrich. Water used for distilled using a EYELA STILL ACE SA-2100A. The reaction at -78°C was carried out using methanol and liquid nitrogen-methanol cooling bath. Spin coating was performed using a MIKASA MS-B 150 spin coater.

S2. General procedure for the preparation of substrates

2-bromo-5-vinylthiophene was prepared by a Wittig reaction from 5-bromo-2-

thiophencarboxyaldehyde according to the previously reported procedure [2].

S2.1. Synthesis of SiVT4

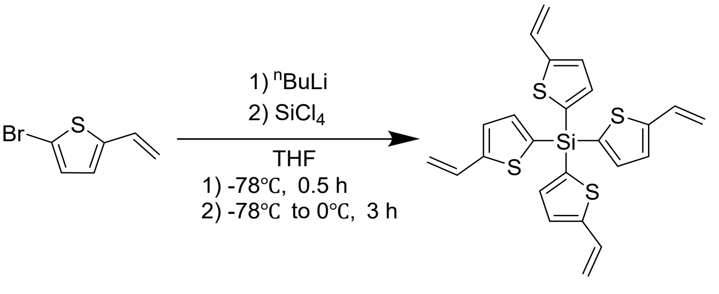

SiVT4

To a two-necked 50 mL flask equipped with a magnetic stirring bar were added 2-bromo-5-vinylthiophene (1.00 g, 5.46 mmol) and THF (30 mL) under N_2 atmosphere. The solution was cooled to -78°C, and *n*-butyllithium (1.6 M in hexane, 3.41 mL, 5.46 mmol) was added dropwise. The reaction mixture was stirring for 0.5 h, then cooled again to -78°C before tetrachlorosilane (125 µL, 1.09 mmol) was added. The mixture was allowed to warm to 0°C and stirring for 3 h. The reaction was quenched with H_2O at -50°C after added TEMPO (0.85 mg, 0.00546 mmol), and the resulting mixture was extracted with EtOAc and brine (3 ×). The organic layer was dried over $MgSO_4$, filtered, and concentrated under reduced pressure at 25°C. The residue was purified by column chromatography in silica gel (hexane) to afford a white solid (467 mg, 92% yield). HRMS (APCI) m/z $[M + H]^+$ calcd. for $C_{24}H_{21}S_4Si$ 465.0290, found 465.0265; ^{1}H NMR (500 MHz, DMSO-*d*$_6$, r.t.) δ 7.37 (d, J =3.51 Hz, 4H), 7.31 (d, J = 3.51 Hz, 4H), 6.95 (dd, J = 17.4, 10.9 Hz, 4H), 5.66 (d, J = 17.5 Hz, 4H), 5.26 (d, J = 11.4Hz, 4H); ^{13}C{^{1}H} NMR (126 MHz, DMSO-*d*$_6$, r.t.) δ 150.4, 139.1, 130.9, 129.3, 128.0, 115.6; ^{29}Si NMR (99 MHz, DMSO-*d*$_6$, r.t.) δ -32.3.

S2.2. Synthesis of SiVT3

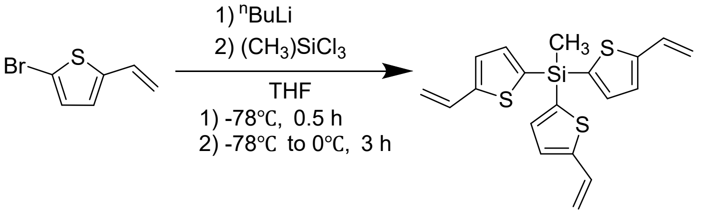

SiVT3

To a two-necked 50 mL flask equipped with a magnetic stirring bar were added 2-bromo-5-vinylthiophene (500 mg, 2.73 mmol) and THF (10 mL) under N_2 atmosphere. The solution was cooled to -78°C, and *n*-butyllithium (1.6 M in hexane, 1.71 mL, 2.73 mmol) was added dropwise. The reaction mixture was string for 0.5 h., then cooled again to -78°C before trichloromethylsilane (91.1 µL, 0.780

mmol) was added. The mixture was allowed to warm to 0°C and stirring for 3 h. The reaction was quenched with H_2O at 0 °C, and the resulting mixture was extracted with EtOAc and brine (3 ×). The organic layer was dried over $MgSO_4$, filtered, and concentrated under reduced pressure at 25°C. The residue was purified by column chromatography in silica gel (hexane) to afford a colorless liquid (179 mg, 62% yield). HRMS (APCI) m/z [M + H]$^+$ calcd. for $C_{19}H_{19}S_3Si$ 371.0413, found 371.0451; ^{1}H NMR (500 MHz, DMSO-d_6, r.t.) δ 7.34 (d, J =3.38 Hz, 3H), 7.25 (d, J = 3.34 Hz, 3H), 6.92 (dd, J = 17.4, 10.9 Hz, 3H), 5.61 (d, J = 17.4 Hz, 3H), 5.22 (d, J = 10.9 Hz, 3H), 0.90 (s, 3H); ^{13}C{^{1}H} NMR (126 MHz, DMSO-d_6, r.t.) δ 149.5, 137.8, 133.3, 129.4, 127.8, 115.0, -1.06; ^{29}Si NMR (99 MHz, DMSO-d_6, r.t.) δ -25.4.

S2.3. Synthesis of SiVT2

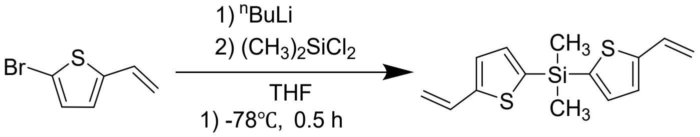

SiVT2

To a two-necked 50 mL flask equipped with a magnetic stirring bar were added 2-bromo-5-vinylthiophene (500 mg, 2.73 mmol) and THF (10 mL) under N_2 atmosphere. The solution cooled to -78°C, and *n*-butyllithium (1.6 M in hexane, 1.71 µL, 2.73 mmol) was added dropwise. The reaction mixture was stirring for 0.5 h, then cooled again to -78°C before chlorodimethylsilane (130 µL, 1.093 mmol) was added. The mixture was allowed to warm to 0°C and stirring for 3 h. The reaction was quenched with H_2O at 0°C, and the mixture was extracted with EtOAc and brine(3 ×). The organic layer was dried over $MgSO_4$, filtered, and concentrated under reduced pressure at 25°C. The residue was purified by column chromatography in silica gel (hexane) to afford a colorless liquid. (250 mg, 83% yield). HRMS (APCI) m/z [M + H]$^+$ calcd. for $C_{14}H_{17}S_2Si$ 277.0535, found 277.0536; ^{1}H NMR (500 MHz, DMSO-d_6, r.t.) δ 7.27 (d, J =3.42 Hz, 2H), 7.20 (d, J = 3.44 Hz, 2H), 6.90 (dd, J = 17.4, 10.9, 2H), 5.57 (d, J = 17.4 Hz, 2H), 5.19 (d, J=10.9 Hz, 2H), 0.56 (s, 6H); ^{13}C{^{1}H} NMR (126 MHz, DMSO-d_6, r.t.) δ 148.5, 136.3, 136.0, 129.5, 127.8, 114.5, -0.739. ^{29}Si NMR (99 MHz, DMSO-d_6, r.t.) δ -15.0.

S2.4. Synthesis of SiVT1

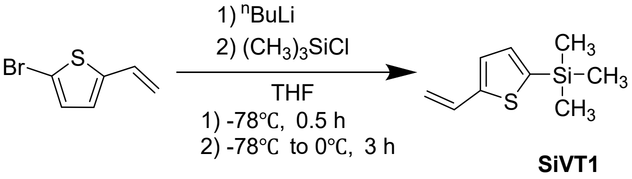

SiVT1

To a two-necked 50 mL flask equipped with a magnetic stirring bar were added 2-bromo-5-

vinylthiophene (500 mg, 2.73 mmol) and THF (10 mL) under N_2 atmosphere. The solution was cooled to -78°C, and *n*-butyllithium (1.6 M in hexane, 1.71 mL, 2.73 mmol) was added dropwise. The reaction mixture was string for 0.5 h., then cooled again to -78°C before chlorotrimethylsilane (276.1 µL, 2.19 mmol) was added. The mixture was allowed to warm to 0°C and stirring for 3 h. The reaction was quenched with H_2O at 0 °C, and the resulting mixture was extracted with EtOAc and brine (3 ×). The organic layer was dried over $MgSO_4$, filtered, and concentrated under reduced pressure at 25°C. The residue was purified by column chromatography in silica gel (hexane) to afford a colorless liquid (343 mg, 86% yield). HRMS (APCI) m/z $[M + H]^+$ calcd. for $C_9H_{15}SSi$ 183.0658, found 183.0629; ^1H NMR (500 MHz, DMSO-d_6, r.t.) δ 7.18 (d, J =3.38 Hz, 1H), 7.16 (d, J = 3.40 Hz, 1H), 6.89 (dd, J = 17.4, 10.8 Hz, 1H), 5.55 (d, J = 17.4 Hz, 1H), 5.17 (d, J = 11.7 Hz, 1H), 0.28 (s, 9H); $^{13}C\{^1H\}$ NMR (126 MHz, DMSO-d_6, r.t.) δ 147.5, 138.9, 135.0, 129.7, 127.6, 113.9, -0.24; ^{29}Si NMR (99 MHz, DMSO-d_6, r.t.) δ -7.71.

S2.5. Synthesis of GeVT4

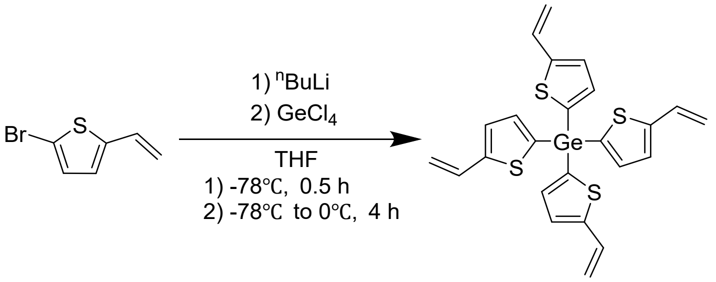

GeVT4

To a two-necked 50 mL flask equipped with a magnetic stirring bar were added 2-bromo-5-vinylthiophene (3.78 g, 21.0 mmol) and THF (30 mL) under N_2 atmosphere. The solution was cooled to -78°C, and *n*-butyllithium (1.6 M in hexane, 12.2 mL, 19.6 mmol) was added dropwise. The reaction mixture was stirring for 0.5 h, then cooled again to -78°C before tetrachlorogermane (12.3 mL, 19.6 mmol) was added. The mixture was allowed to warm to 0°C and stirring for 4h. The reaction was quenched with CH_3OH at 0°C, and the mixture was extracted with CH_2Cl_2 and brine (3 ×). The organic layer was dried with $MgSO_4$, filtered, and evaporated under vacuum. The residue was washed with n-hexane, filtered, and concentrate the filtrate using an evaporator to give tetrakis(5-vinylthiophene-2-yl) germane as white solids (2.05 g, 86% yield). HRMS (APCI) m/z $[M]^+$ calcd for $C_{24}H_{21}S_4Ge$ 510.9732, found 510.9680; ^1H NMR (500 MHz, DMSO-d_6, r.t.) δ 7.32-7.30 (m, 8H), 6.94 (dd, J = 17.4, 10.9 Hz, 4H), 5.63 (d, J = 17.8 Hz, 4H), 5.24 (d, J = 11.4 Hz, 4H); $^{13}C\{^1H\}$ NMR (126 MHz, DMSO-d_6, r.t.) δ 149.3, 137.1, 131.2, 129.2, 127.8, 115.2.

S2.6. Synthesis of SnVT4

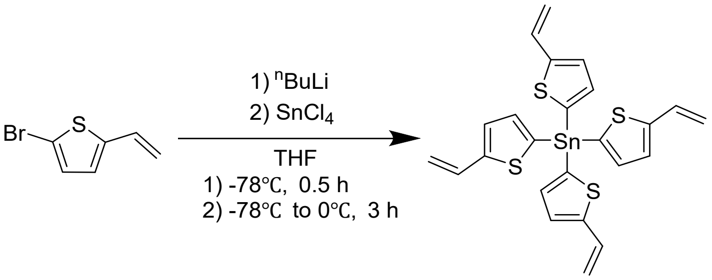

SnVT4

To a two-necked 50 mL flask equipped with a magnetic stirring bar were added 2-bromo-5-vinylthiophene (900 mg, 4.92 mmol) and THF (30 mL) under N_2 atmosphere. The solution was cooled to -78°C, and *n*-butyllithium (1.6 M in hexane, 3.07 mL, 4.92 mmol) was added dropwise. The reaction mixture was stirring for 0.5 h, then cooled again to -78°C before tin(IV) chloride (180 µl, 0.983 mmol) was added. The mixture was allowed to warm to 0°C and stirring for 3 h. The reaction was quenched with H_2O at -50°C after added TEMPO (0.77 mg, 0.00492 mmol), and the resulting mixture was extracted with EtOAc and brine (3 ×). The organic layer was dried over $MgSO_4$, filtered, and concentrated under reduced pressure at 25°C. The residue was purified by column chromatography in silica gel (hexane) to afford a white solid (134.4 mg, 25% yield). HRMS (APCI) m/z $[\mathrm{M+H}]^+$ calcd. for $C_{24}H_{21}S_4Sn$ 556.9543, found 556.9541; ^{1}H NMR (500 MHz, DMSO-d_6, r.t.) δ 7.30 (d, J =6.07 Hz, 8H), 6.95 (dd, J = 16.5, 11.7 Hz, 4H), 5.61 (d, J = 17.4, 4H), 5.21 (d, J = 10.8 Hz, 4H); ^{13}C{^{1}H} NMR (126 MHz, DMSO-d_6, r.t.) δ 149.3, 138.2, 133.2, 129.4, 127.6, 114.5.

S2.7. Preparation of polymer film by thermal radical polymerization

A mixture of **SiVT4** (0.116 g, 0.25 mmol), ADVN (0.062 mg, 0.00025 mmol) and toluene (250 µL) were placed in a dry 10 mL flask, and then the solution was degassed by three freeze-evacuate-thaw cycles. After the solution was sandwiched between two glass plates with 300 µm Teflon sheet as a spacer and cured by heating at 60°C for 24 h (**Figure S1**).

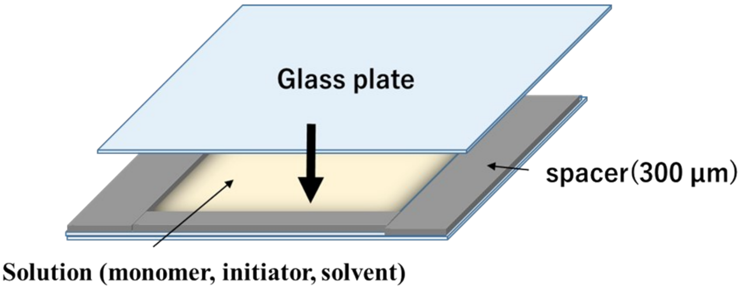

Figure S1. Schematic image of curing process.

S2.8. Copolymerization of NMT-A with SiVT4

Copolymerization of NMT-A with **SiVT4** was carried out in the spin-coated film of mixture. A thin film of the NMT-A/ **SiVT4** mixture (0.2 µL, 3000 rpm, 20 s) was cured at 100℃ for 1 h a nitrogen atmosphere to obtain the polymer. Polymerization was performed for three different formulations; NMT-A alone (Entry 1), NMT-A with 10 wt% **SiVT4** (Entry 2), and NMT-A with 20 wt% **SiVT4** (Entry 3). For entry1, 500 mg of NMT-A was mixed with 5 mg of ADVN (initiator) and 1.5 mg of BYK-307 (leveling agent). Entry 2 consisted of 220 mg of NMT-A, 24,4 mg of **SiVT4**, 2.44 mg of ADVN, and 0.73 mg of BYK-307. Finally, Entry 3 contained 200 mg of NMT-A, 50 mg of **SiVT4**, 2.5 mg of ADVN, and 0.75 mg of BYK-307.

S3. Refractive index measurements

S3.1. Refractive index measurement of SiVT1–SiVT4, GeVT4 and SnVT4

The liquid monomers **SiVT1**, **SiVT2** and **SiVT3** were measured directly using an abbe refractometer at the Sodium D line (589 nm). Since **SiVT4**, **GeVT4** and **SnVT4** are solids, mixtures with NMT-A were prepared. The refractive indices of neat NMT-A and mixtures containing 10 wt% and 20 wt% of each compound were measured. All Values are reported as mean ± standard deviation from four independent measurements (n= 4). The refractive index showed a linear dependence on composition, and the refractive index of the pure compound was obtained by linear extrapolation to 100 wt%.

The refractive index of neat NMT-A was 1.60 (±0.0000). For **SiVT4**, mixtures containing 10 wt% and 20 wt% **SiVT4** were 1.61 (±0.0008) and 1.61 (±0.0022), and linear extrapolation gave an estimated value of 1.68 for the pure **SiVT4** (**Figure S2**). For **GeVT4**, mixtures containing 10 wt% and 20 wt% **GeVT4** in NMT-A were 1.61 (±0.0008) and 1.62 (±0.0022), and linear extrapolation gave an estimated refractive index of 1.68 for pure **GeVT4** (**Figure S3**). For **SnVT4**, mixtures containing 10 wt% and 20 wt% in NMT-A were 1.60 (±0.0008) and 1.61 (±0.0008), and linear extrapolation gave an estimated refractive index of 1.69 for pure **SnVT4** (**Figure S4**).

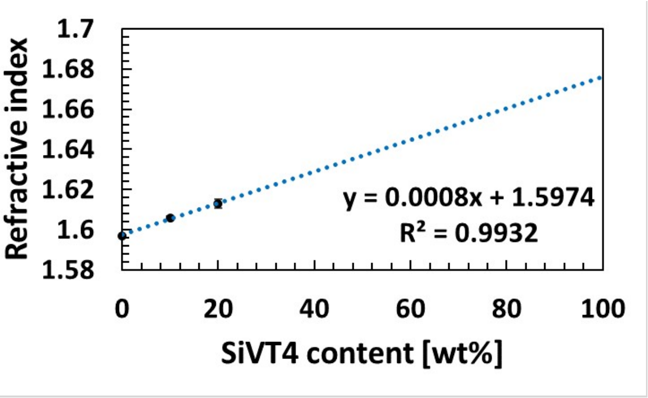

Figure S2. Refractive index of NMT-A/**SiVT4** mixtures as a function of **SiVT4** content

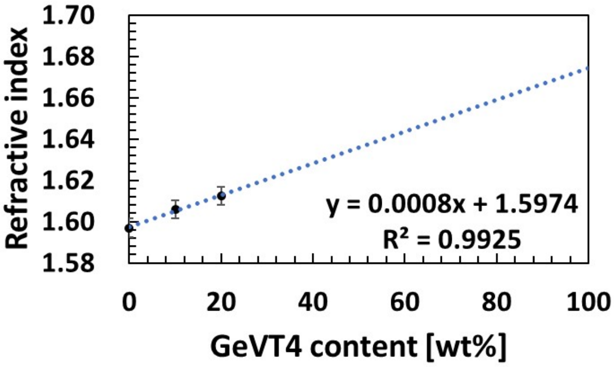

Figure S3. Refractive index of NMT-A/**GeVT4** mixtures as a function of **GeVT4** content

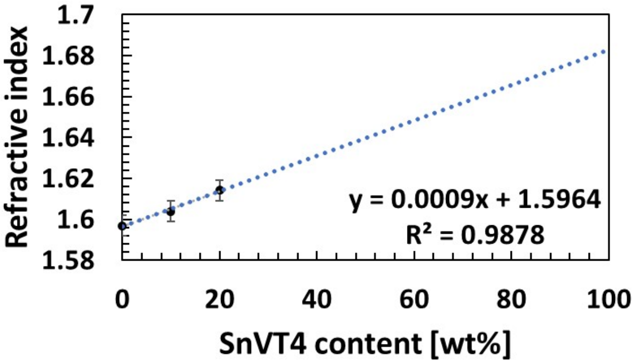

Figure S4. Refractive index of NMT-A/**SnVT4** mixtures as a function of **SnVT4** content

S3.2. Discussion of Refractive Indices in Thermally Cured Polymers

To better understand the origin of the refractive-index enhancement in SiVT4-containing formulations, refractive indices before and after thermal curing were compared.

Neat NMT-A showed an increase in refractive index from 1.60 to 1.62 after curing at 100 °C for 1 h. In comparison, the formulation containing 10 wt% SiVT4 increased from 1.60 to 1.67, while that containing 20 wt% SiVT4 increased from 1.61 to 1.68.

These results show that the enhancement develops through two contributions: incorporation of SiVT4 into the uncured formulation maintains or slightly increases refractive index, and subsequent curing leads to a much larger increase than observed for neat NMT-A alone. This behavior indicates that the high refractive-index performance arises from the cooperative effects of the SiVT4 molecular structure, namely its intrinsically high molar refraction together with efficient network formation during curing.

To better understand the origin of the refractive-index enhancement in SiVT4-containing formulations, the refractive indices before and after thermal curing were compared using the samples described above. Neat NMT-A showed an increase in refractive index from 1.60 to 1.62 after curing at 100 °C for 1 h. In comparison, the formulation containing 10 wt% SiVT4 increased from 1.60 to 1.67, while that containing 20 wt% SiVT4 increased from 1.61 to 1.68.

These results show that the enhancement develops in two contributions: incorporation of SiVT4 into the uncured formulation maintains or slightly increases refractive index, and subsequent curing leads to a much larger increase than observed for neat NMT-A alone. This behavior indicates that the high refractive-index performance arises from the cooperative effects of the SiVT4 molecular structure, namely its intrinsically high molar refraction together with efficient network formation during curing.

S4. ^{1}H NMR, ^{13}C NMR and ^{29}Si NMR spectra

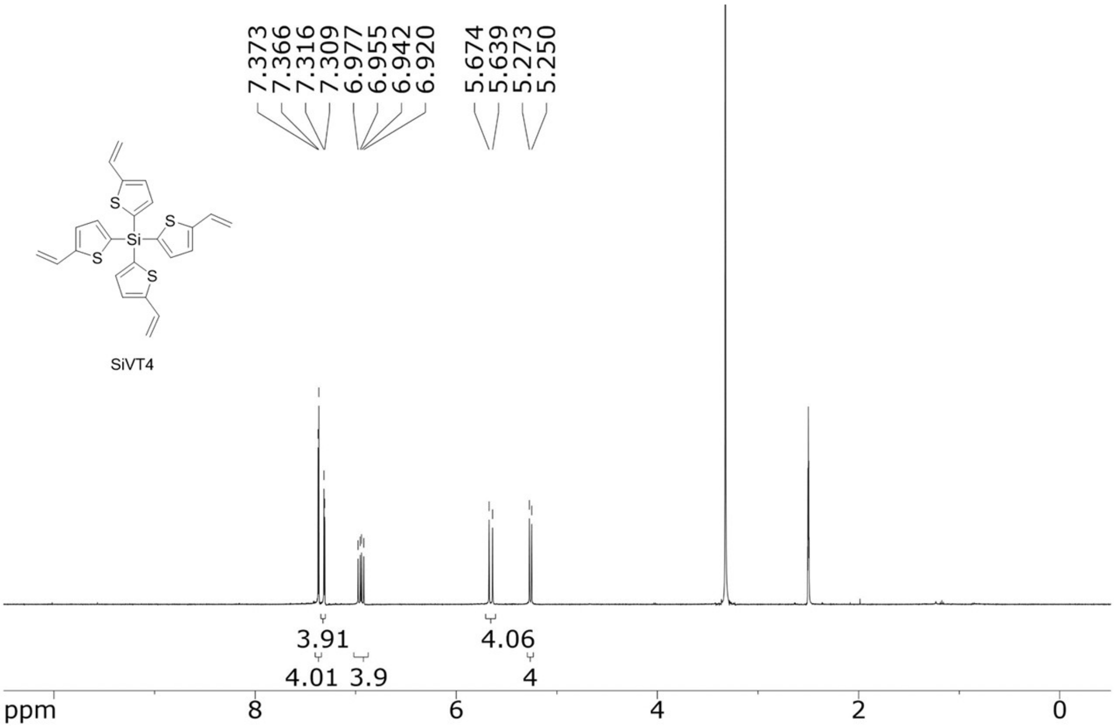

Figure S5. ^{1}H NMR spectrum of **SiVT4** (500 MHz, DMSO-d_6, r.t.)

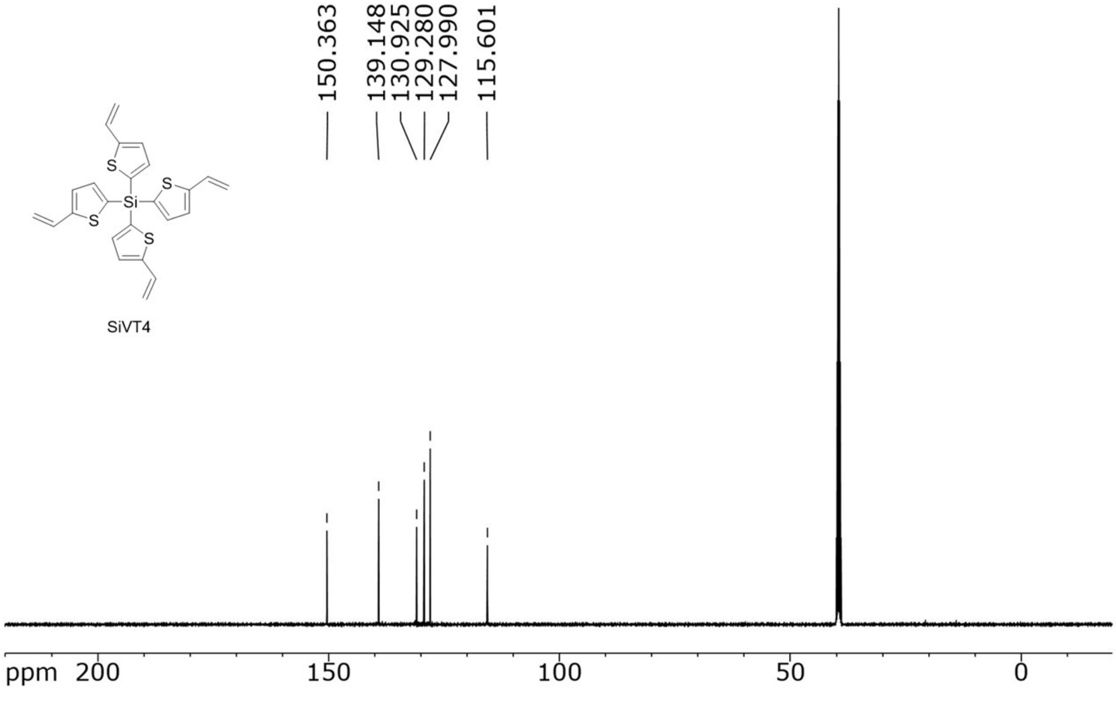

Figure S6. ^{13}C{^{1}H} NMR spectrum of **SiVT4** (126 MHz, DMSO-d_6, r.t.)

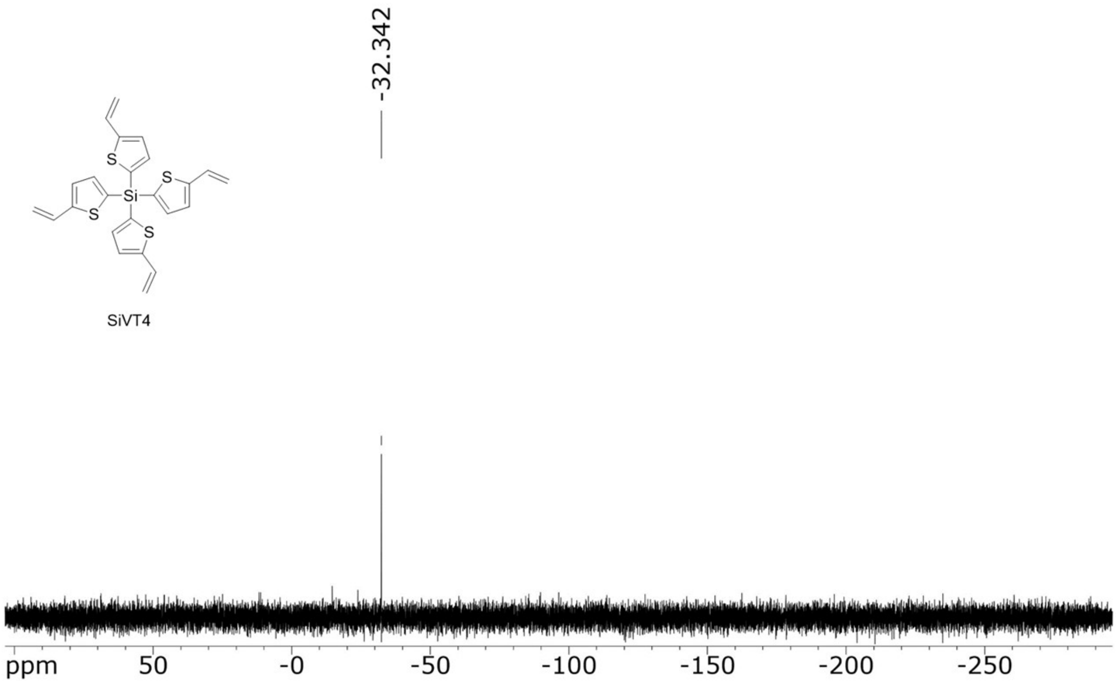

Figure S7. $^{29}Si\{^{1}H\}$ NMR spectrum of **SiVT4** (99 MHz, DMSO-d_6, r.t.)

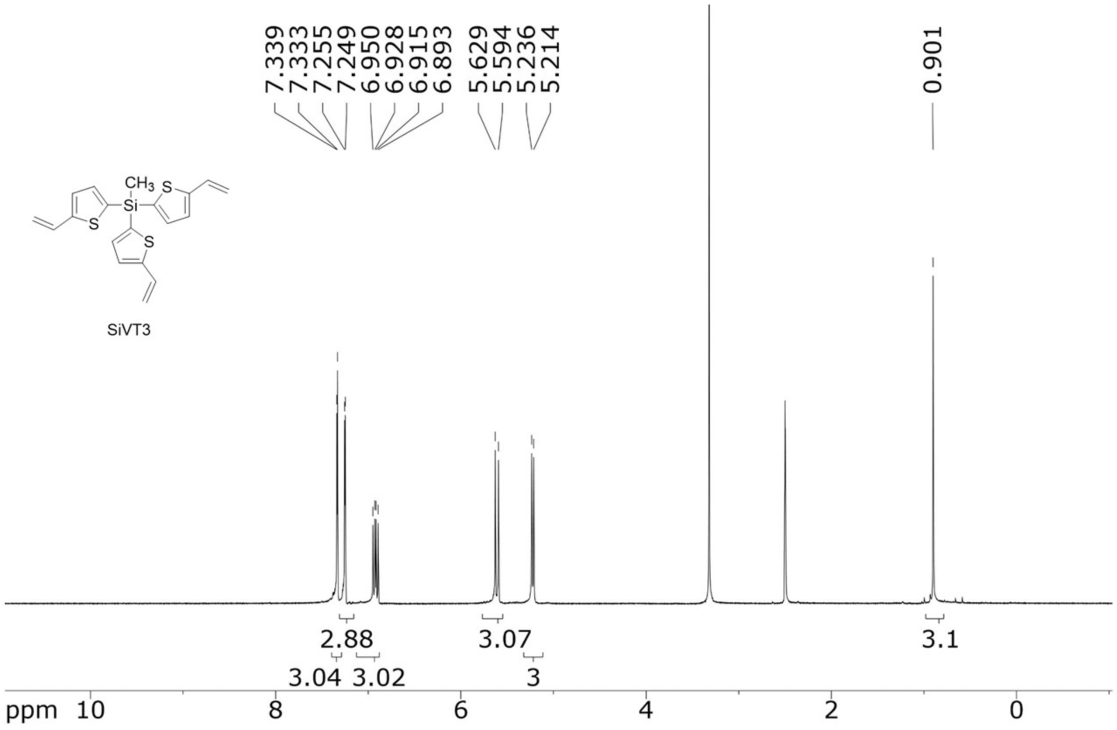

Figure S8. ^{1}H NMR spectrum of **SiVT3** (500 MHz, DMSO-d_6, r.t.)

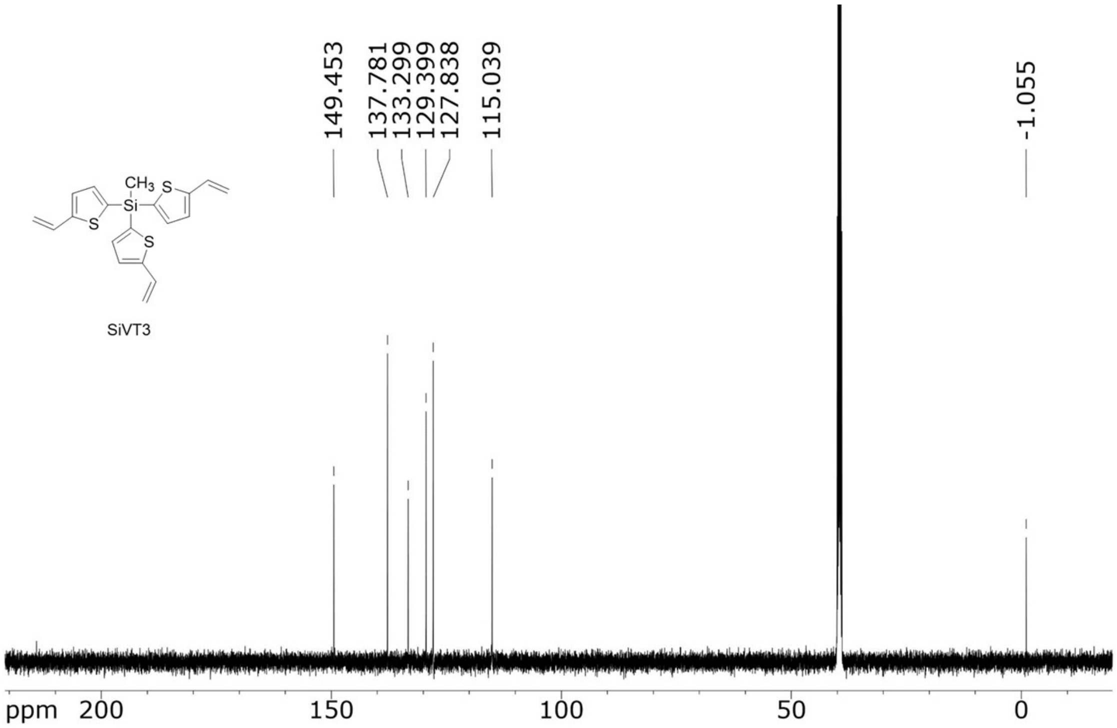

Figure S9. $^{13}C\{^1H\}$ NMR spectrum of **SiVT3** (126 MHz, DMSO-d_6, r.t.)

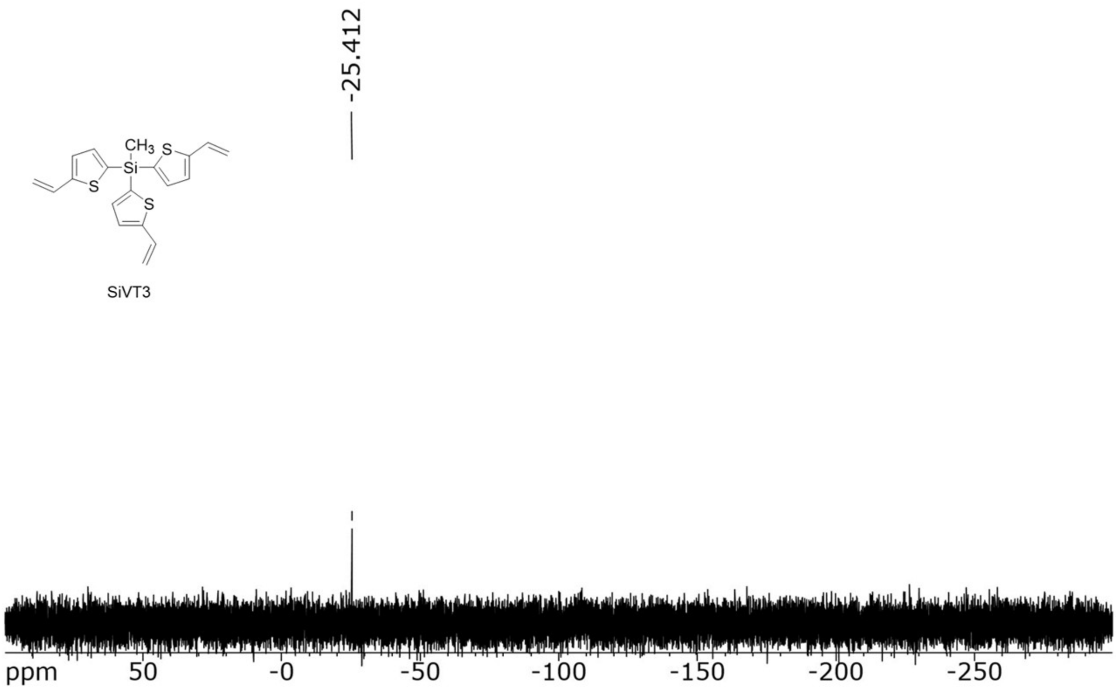

Figure S10. $^{29}Si\{^1H\}$ NMR spectrum of **SiVT3** (99 MHz, DMSO-d_6, r.t.)

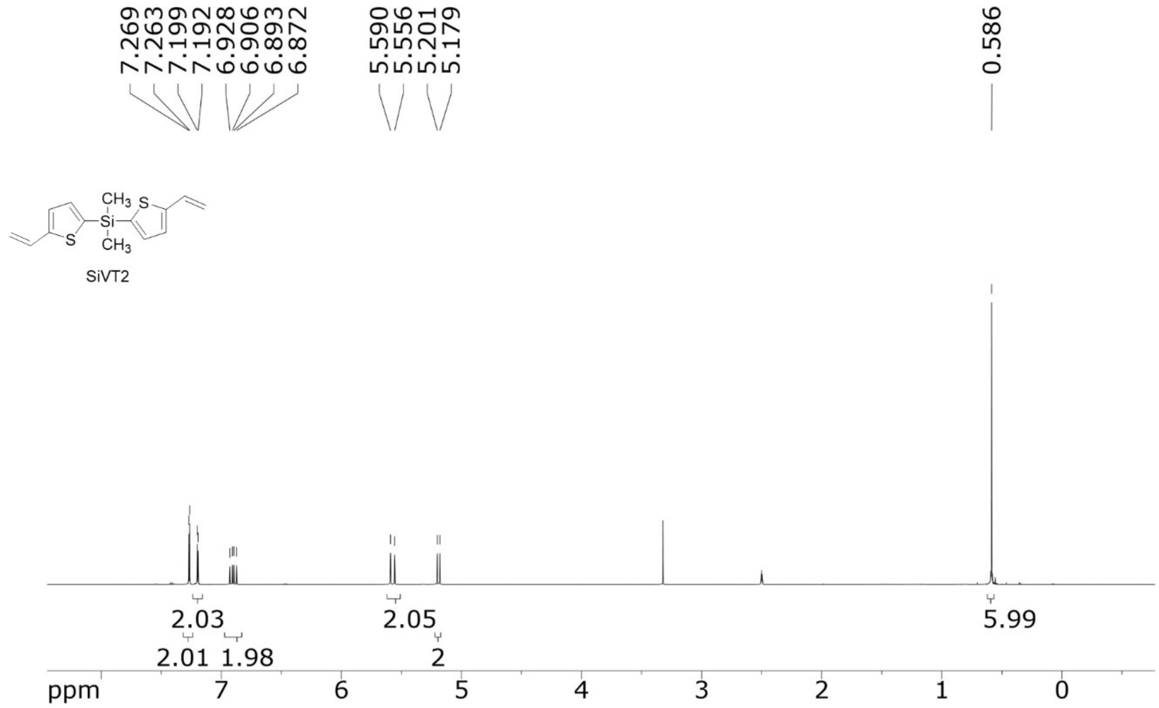

Figure S11. ^{1}H NMR spectrum of **SiVT2** (500 MHz, DMSO-d_6, r.t.)

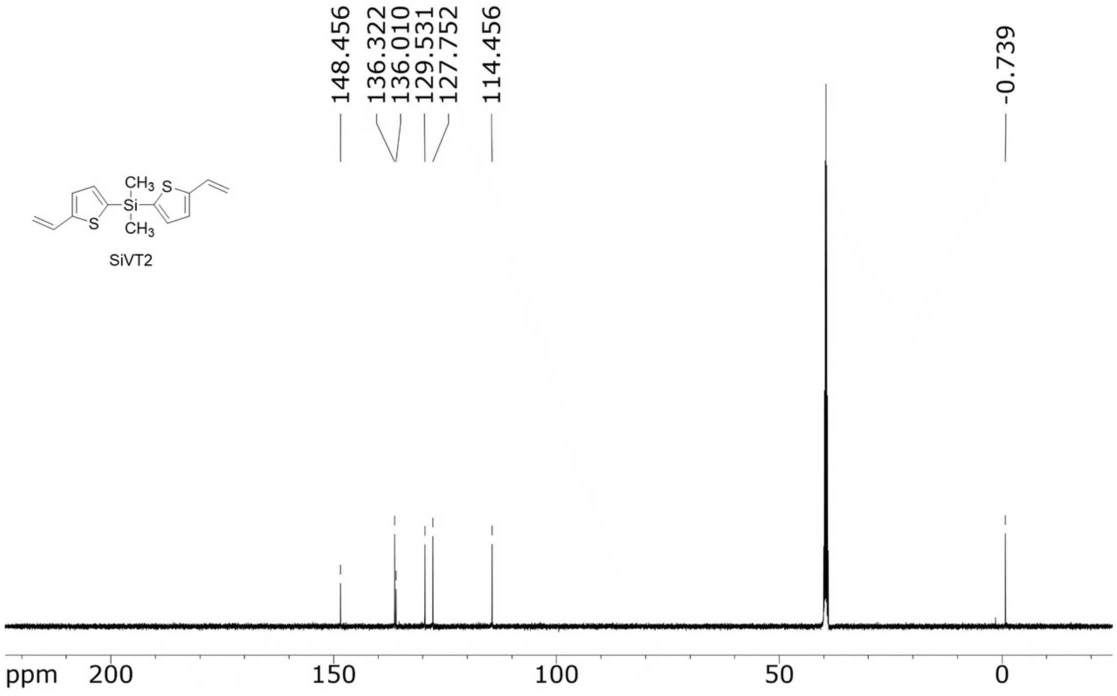

Figure S12. ^{13}C{^{1}H} NMR spectrum of **SiVT2** (126 MHz, DMSO-d_6, r.t.)

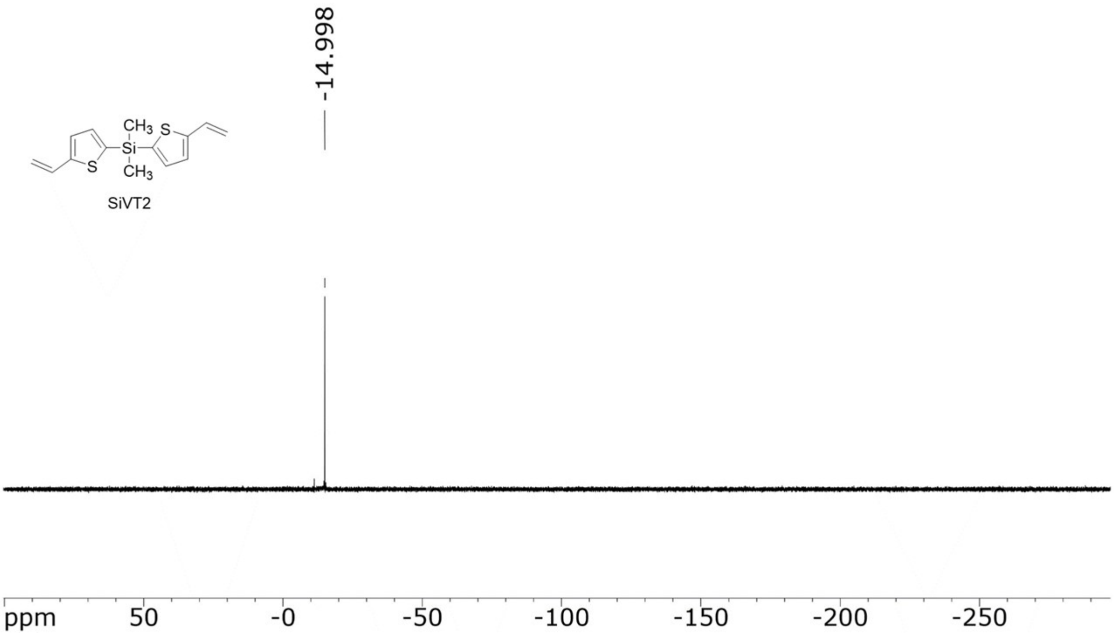

Figure S13. $^{29}Si\{^1H\}$ NMR spectrum of **SiVT2** (99 MHz, DMSO-d_6, r.t.)

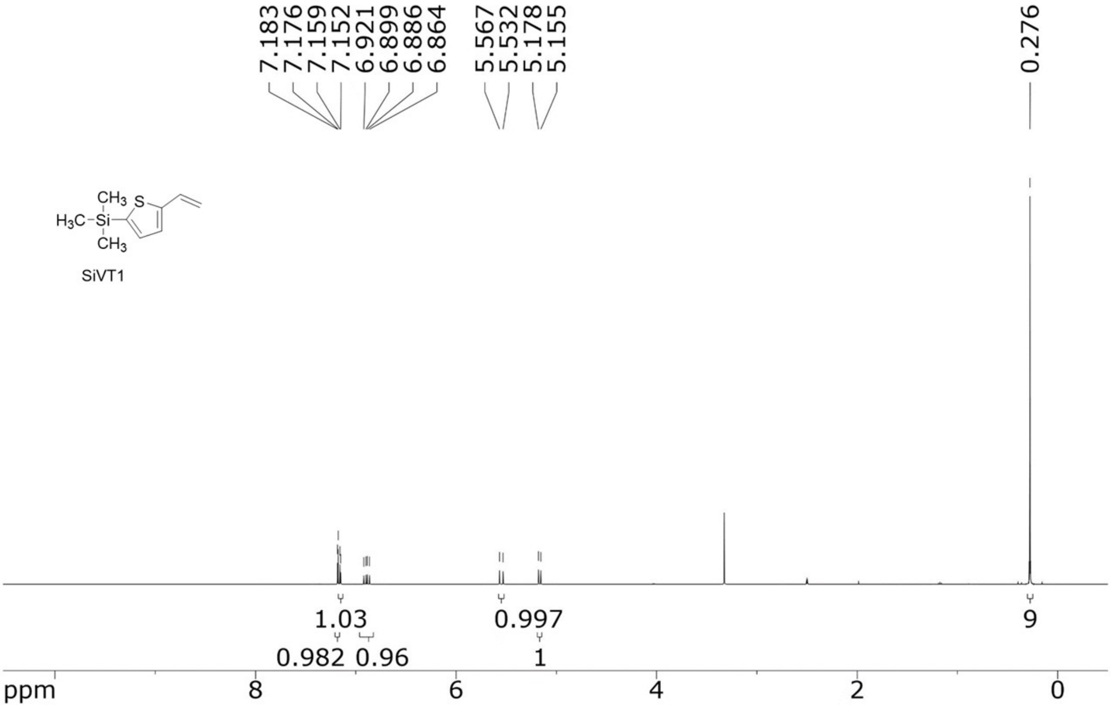

Figure S14. ^1H NMR spectrum of **SiVT1** (500 MHz, DMSO-d_6, r.t.)

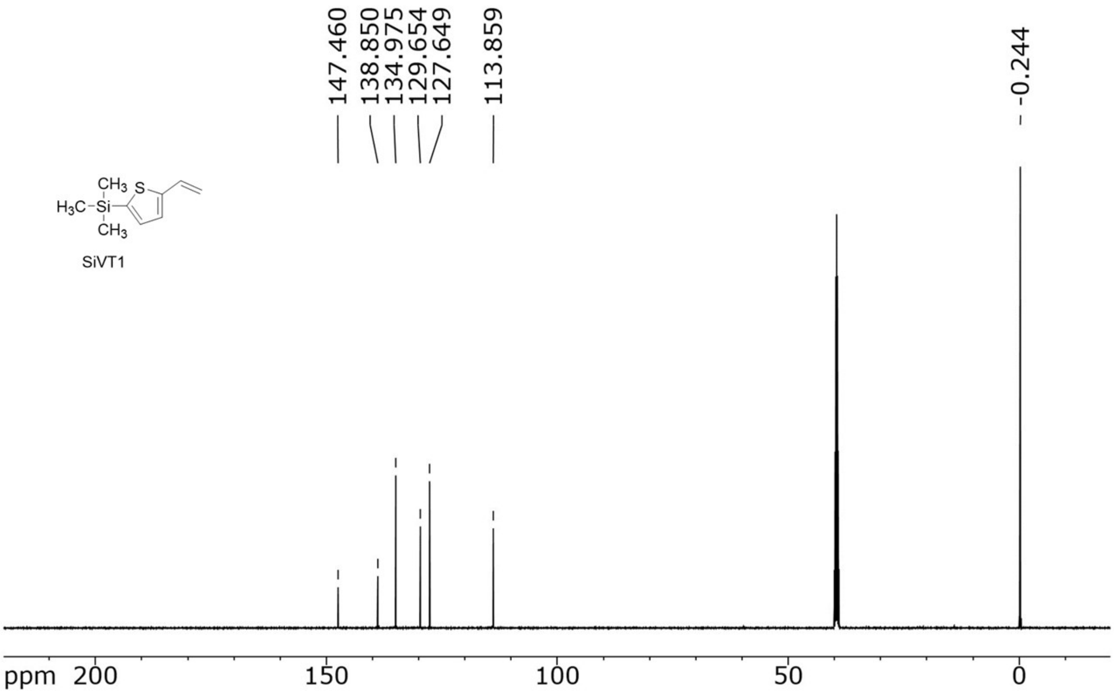

Figure S15. $^{13}C\{^{1}H\}$ NMR spectrum of **SiVT1** (126 MHz, DMSO-d_6, r.t.)

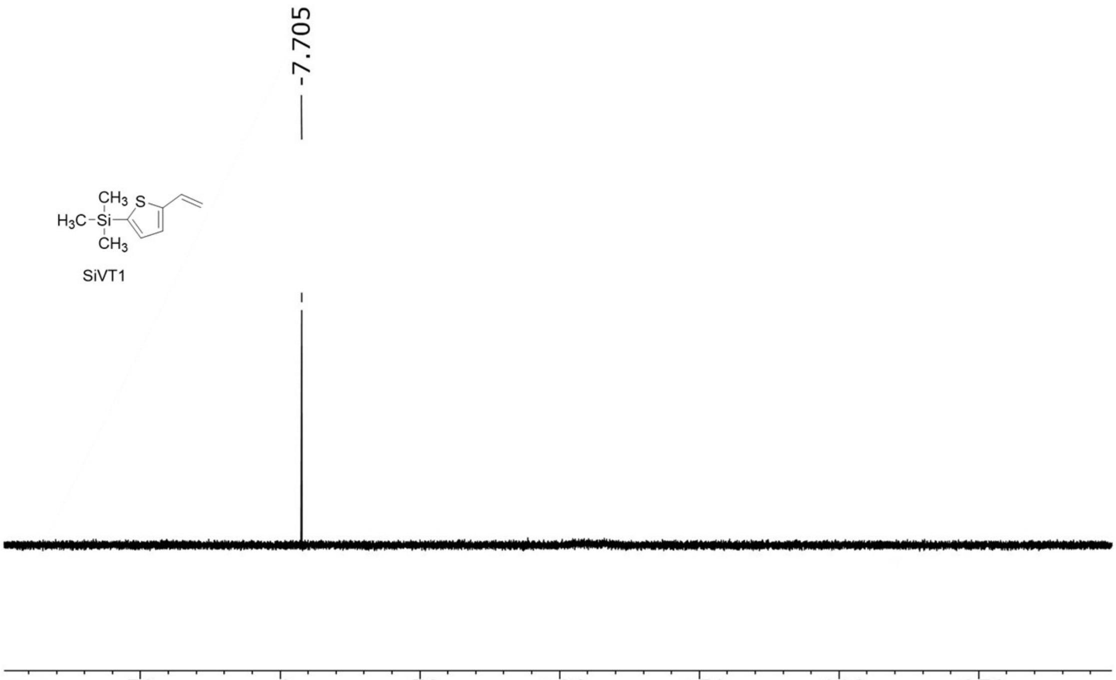

Figure S16. $^{29}Si\{^{1}H\}$ NMR spectrum of **SiVT1** (99 MHz, DMSO-d_6, r.t.)

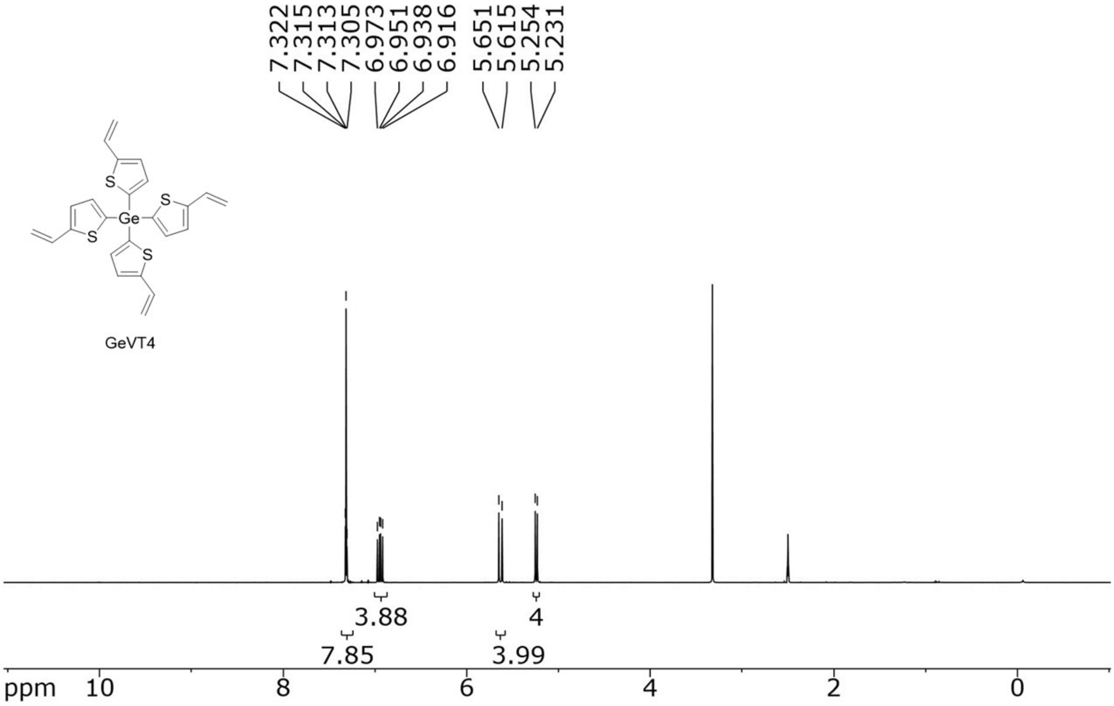

Figure S17. ^{1}H NMR spectrum of **GeVT4** (500 MHz, DMSO-d_6, r.t.)

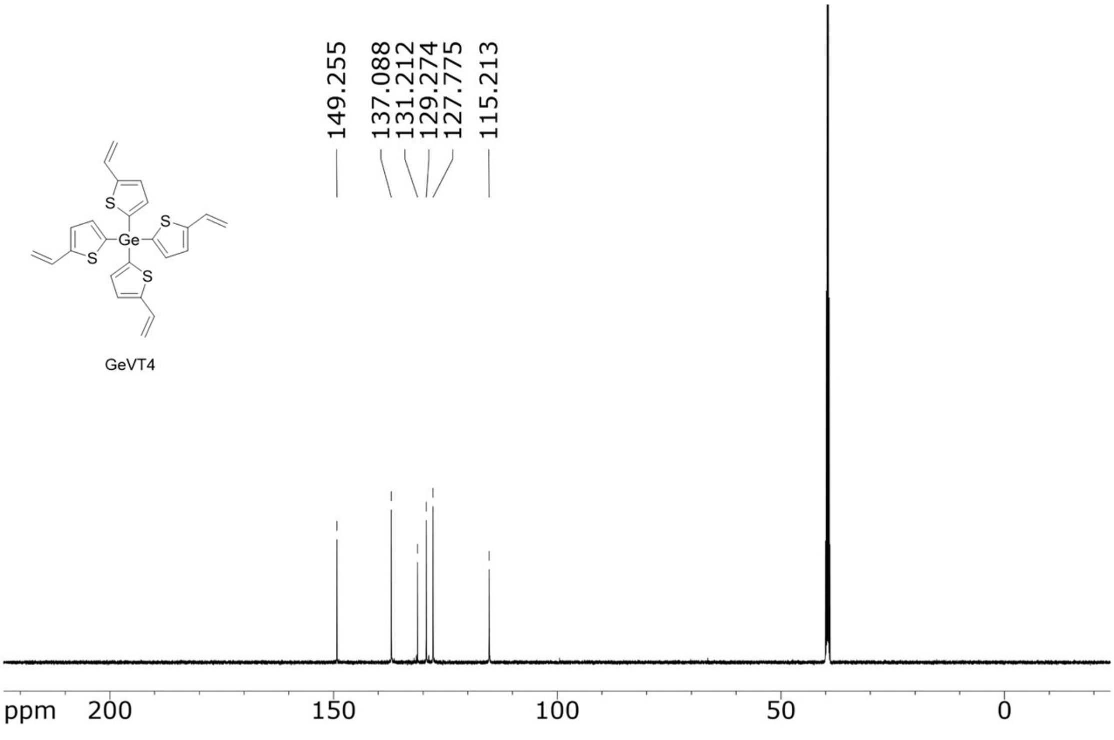

Figure S18. ^{13}C{^{1}H} NMR spectrum of **GeVT4** (126 MHz, DMSO-d_6, r.t.)

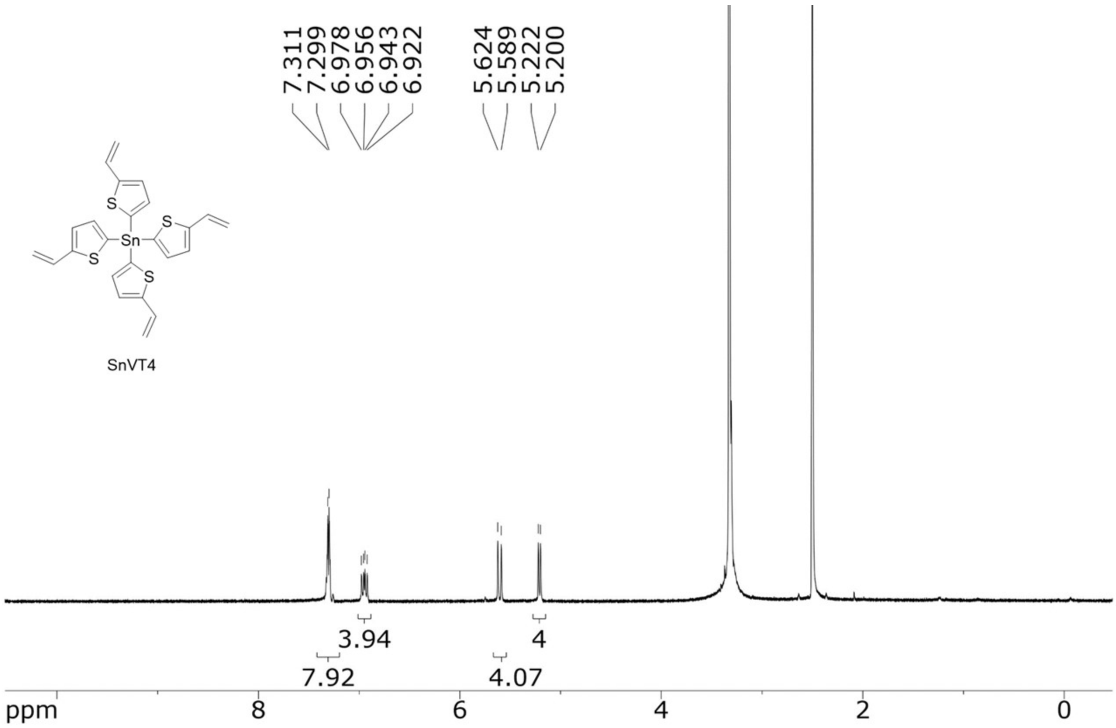

Figure S19. ^{1}H NMR spectrum of **SnVT4** (500 MHz, DMSO-d_6, r.t.)

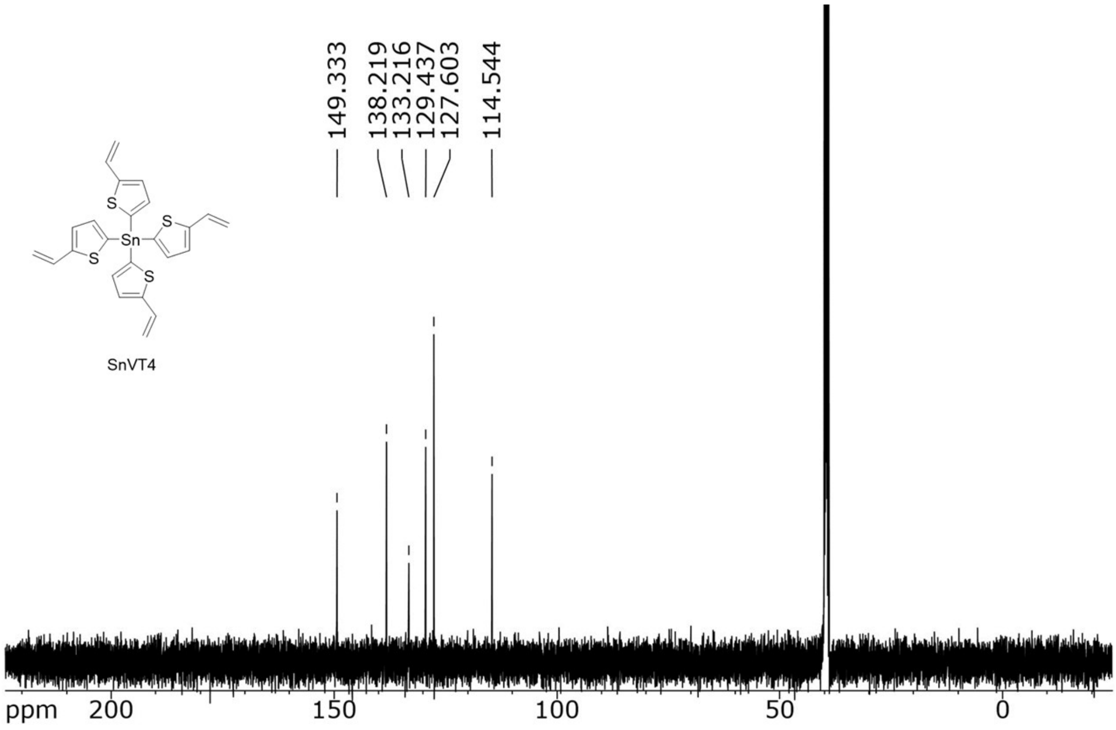

Figure S20. ^{13}C{^{1}H} NMR spectrum of **SnVT4** (126 MHz, DMSO-d_6, r.t.)

S5. APCI-MS spectra

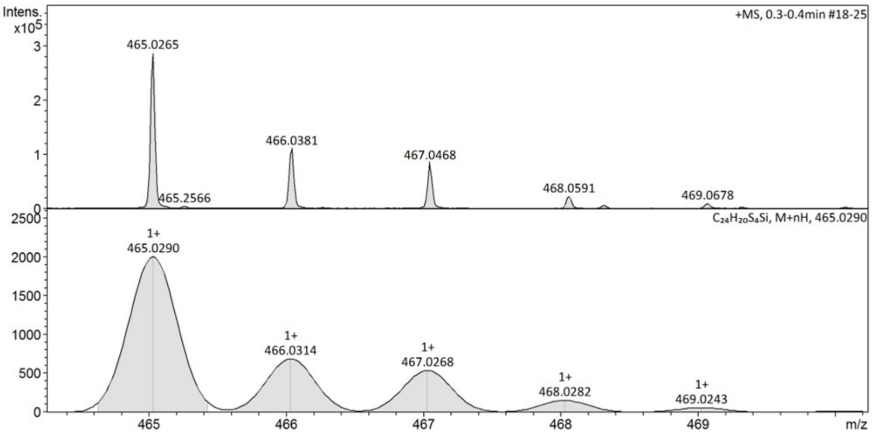

Figure S21. HR-MS spectrum of **SiVT4** (top) with the calculated isotopic distribution (bottom).

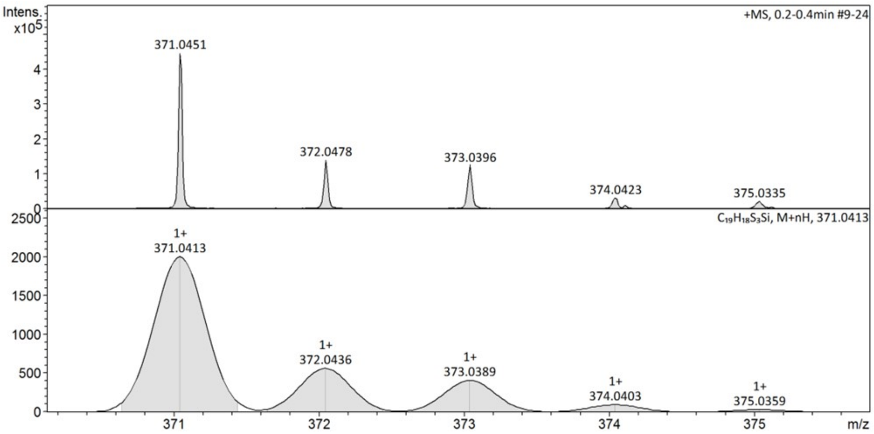

Figure S22. HR-MS spectrum of **SiVT3** (top) with the calculated isotopic distribution (bottom).

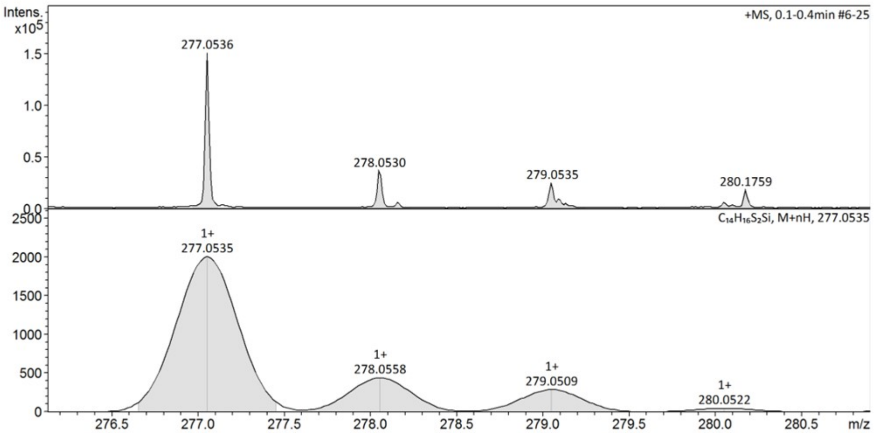

Figure S23. HR-MS spectrum of **SiVT2** (top) with the calculated isotopic distribution (bottom).

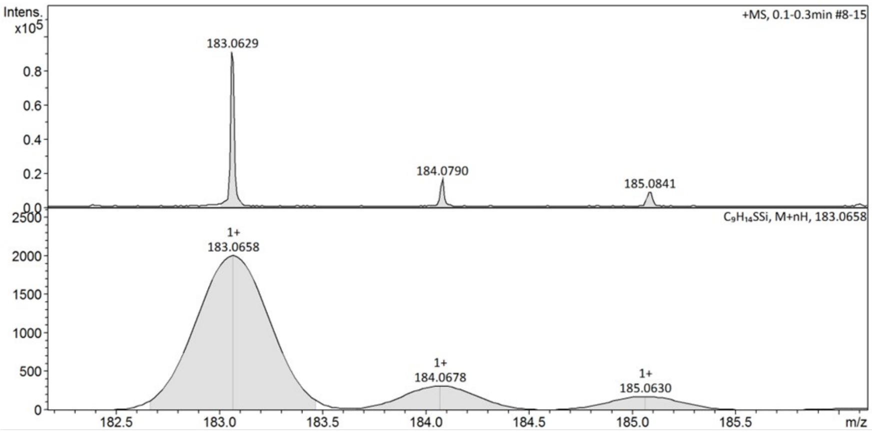

Figure S24. HR-MS spectrum of **SiVT1** (top) with the calculated isotopic distribution (bottom).

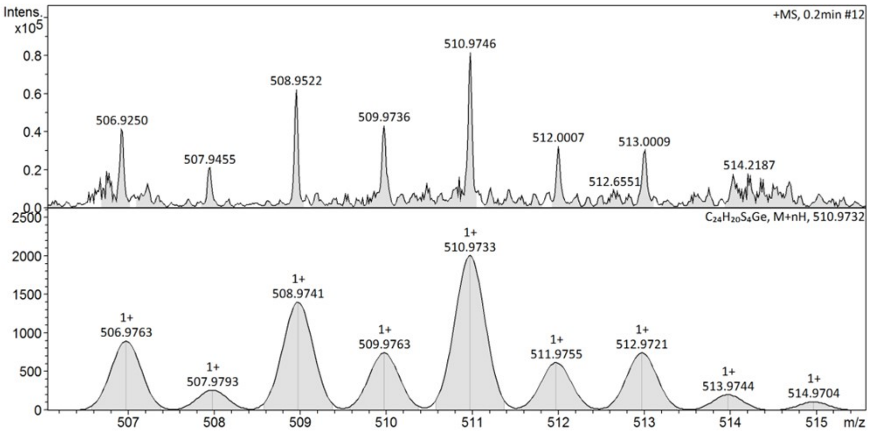

Figure S25. HR-MS spectrum of **GeVT4** (top) with the calculated isotopic distribution (bottom).

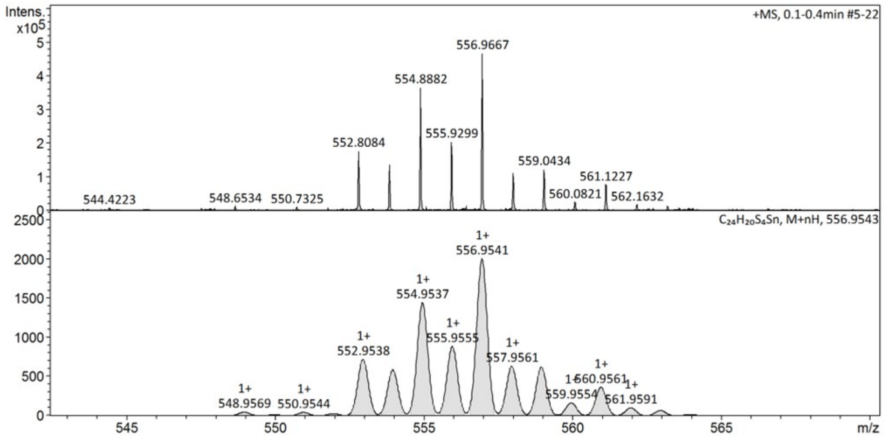

Figure S26. HR-MS spectrum of **SnVT4** (top) with the calculated isotopic distribution (bottom).

S6. ATR-IR Spectral Analysis and Discussion

As described in the main text, the characteristic C=C stretching band of the vinyl group at 1617 cm^{-1} decreased after polymerization, accompanied by the appearance of an aliphatic C–H stretching band at 2919 cm^{-1}. In this section, we discuss the newly emerged peak observed around 1700 cm^{-1}, which was not addressed in the main text (**Figure S27**).

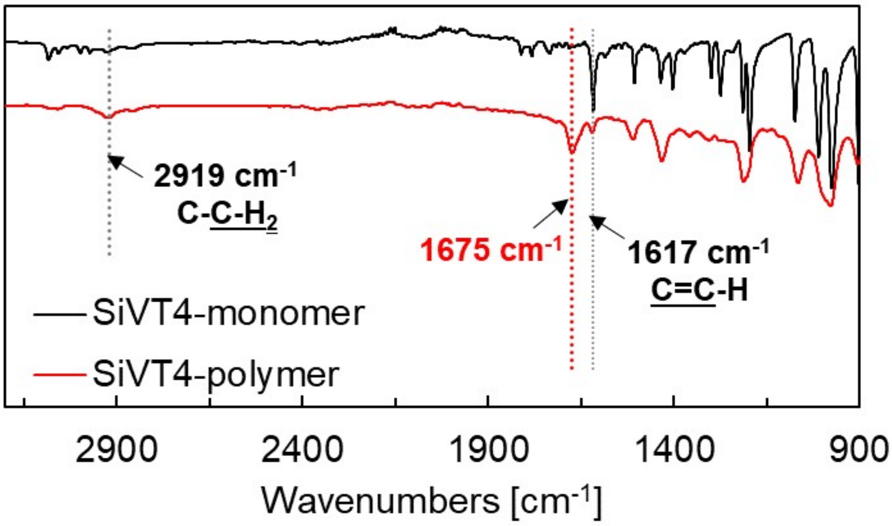

Figure S27. ATR spectra of SiVT4 and its corresponding polymer

The newly observed vibrational band around 1675 cm^{-1} in the ATR-IR spectrum is tentatively attributed to constrained vibrational modes of carbon–carbon bonds and valence angles in aromatic fragments within the highly crosslinked network. Similar features have been reported in hyper-crosslinked polystyrene systems, where such bands arise from structural constraints rather than carbonyl functionalities. Although a minor contribution from trace oxidative species cannot be completely excluded, the dominant origin is considered to be associated with the rigid and highly interconnected polymer structure.[3,4]

S7. Computational details

S7.1. TD-DFT calculation of SiVT1–4, GeVT4 and SiVT4 dimer

TD-DFT calculations were performed using the Gaussian 16 software.[4] The molecular structures of **SiVT4**, **SiVT3**, **SiVT2**, **SiVT1**, **GeVT4** and **SiVT4 dimer** used in TD-DFT calculations were optimized at the cam-B3LYP[5]/6-311+G(d,p) level. Frequency calculations were performed at the same calculation level. TD-DFT calculations were performed using cam-B3LYP functional. The longest-wavelength absorption bands of **SiVT1–4** and **GeVT4** correspond to S0 → S1 electronic transitions and are shown in **Table S1**. In addition, to clarify the origin of the UV–vis absorption characteristics observed for the polymer (Fig. 3d), TD-DFT calculations were performed using the **SiVT4 dimer** as a model compound. All calculated transitions of the **SiVT4** monomer and dimer are summarized in **Table S2** and **Table S3**, respectively. For the monomer, the lowest-energy absorption band is mainly composed of several closely spaced excited states (S1–S3), each of which exhibits a significant oscillator strength. In addition, several higher-energy transitions with relatively small oscillator strengths are also observed. In contrast, the **SiVT4 dimer** shows a larger number of excited states within a similar energy range, together with a redistribution of oscillator strengths among these transitions. As a result, the electronic state density in the same spectral region increases compared to the monomer, which is consistent with the experimentally observed broadened and structured absorption band.

Table S1. The first transitions of **SiVT1–4** and **GeVT4** by TD-DFT at the cam-B3LYP/6-311+G(d,p) level

Compound	Wavelength [nm]	Oscillator strength [f]	HOMO -LUMO gap energy [eV]
SiVT4	282.03	0.2717	6.922
SiVT3	278.15	0.7192	7.072
SiVT2	277.47	0.7228	7.014
SiVT1	272.25	0.4266	7.132
GeVT4	279.00	0.3038	6.942

Table S2. The all transitions of **SiVT4** by TD-DFT at the cam-B3LYP/6-311+G(d,p) level

State	Wavelength [nm]	Oscillator strength [f]
S1	282.03	0.2717
S2	276.69	0.5150
S3	277.92	1.0076
S4	262.70	0.0656
S5	242.29	0.0418
S6	241.79	0.0380
S7	241.13	0.0583
S8	239.16	0.0487

Table S3 The all transitions of **SiVT4 dimer** by TD-DFT at the cam-B3LYP/6-311+G(d,p) level

State	Wavelength [nm]	Oscillator strength [f]
S1	277.41	0.4941
S2	275.26	0.3725
S3	274.01	0.6815
S4	263.28	0.6741
S5	263.89	0.6339
S6	260.60	0.2412
S7	240.05	0.0244
S8	238.81	0.0331
S9	238.50	0.0282
S10	238.11	0.0487

S7.2. Calculated molecular refractive index of vinylthiophene unit

The molar refraction$[R]$ was evaluated using the Lorentz-Lorenz equation (1):

$$\frac{{n_D}^2-1}{{n_D}^2+2}=\frac{4\pi\rho N_A}{3\ M_W}\alpha=\frac{[R]}{V_0}\#(1)$$

where n_D is the refractive index at the D-line, ρ is the density, N_A is the Avogadro constant, α is the molecular polarizability, M_W is the molecular weight, $[R]$ is the molar refraction, and V_0 is the molecular volume.

First, the theoretical molar refraction of **SiVT1–SiVT4** was calculated from the polarizability (α) based on Equation (2) (**Table S4**).

$$[R]=\frac{4\pi}{3}N_A\alpha\#(2)$$

A linear correlation was observed where the polarizability decreased by approximately 12 Å^3 per vinylthiophene unit, corresponding to a molar refraction of 30.26 cm^3 mol^{-1} per unit.

Second, the experimental molar refraction was determined using the measured refractive index (n_D) and the calculated molecular volume (V_0) based on Equation (3).

$$n_D=\sqrt{\frac{1+\frac{2[R]}{V_0}}{1-\frac{[R]}{V_0}}}\#(3)$$

. A discrepancy between the calculated and experimental $[R]$ values was observed, likely due to the inherent sensitivity and deviations in the calculated molecular volume.

Furthermore, the molar refractions of SiVT4, GeVT4, and SnVT4 were compared at a unified level of theory (CAM-B3LYP/LANL2DZ). As a result, the trend in the theoretical molar refraction calculated from the polarizability based on Equation (2) was consistent with the trend observed in the experimentally measured refractive indices (**Table S5**).

Table S4. Calculated polarizability, molecular volume at the cam-B3LYP/6-311+G(d,p) level, and predicted molar refraction

	SiVT4	SiVT3	SiVT2	SiVT1
Calc. α / Å^3	59.35	47.29	34.73	22.53
$[R]$ from Calc. α / cm^3 mol^{-1}	149.68	119.27	87.60	56.82
Measured n_D	1.58	1.61	1.65	1.69
Calc. V_0 / cm^3 mol^{-1}	340.294	264.939	273.029	109.736
$[R]$ from Calc. V_0 / cm^3 mol^{-1}	113.25	91.86	99.58	41.94

Table S5. Calculated polarizability, molecular volume at the cam-B3LYP/LANL2DZ level, and predicted molar refraction

	SiVT4	**GeVT4**	**SnVT4**
Calc. α / Å^3	50.66	50.78	54.07
$[R]$ from Calc. α / cm^3 mol^{-1}	127.74	127.96	136.26
Measured n_D	1.68	1.68	1.69
Calc. V_0 / cm^3 mol^{-1}	360.31	296.14	340.67
$[R]$ from Calc. V_0 / cm^3 mol^{-1}	136.28	111.9	122.25

S7.3. Calculated structures and Cartesian coordinates

SiVT4

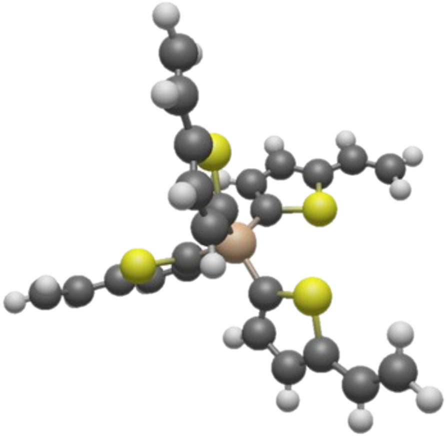

0 1

Si	-0.11240400	-0.16612800	-0.21867800
C	0.47927200	1.76593500	-2.30621800
S	2.66026300	0.90078800	-1.30933800
C	2.76738000	2.11128200	-2.54403200
C	-1.62868000	-0.68845000	-1.17132800
C	-1.71744200	-1.01858000	-2.49789800
S	-3.16935800	-0.90611800	-0.40467100
C	-3.00903300	-1.44613500	-2.89521500
H	-0.87600700	-0.95147800	-3.17520900
C	-3.91734300	-1.44436000	-1.87161400
H	-3.26625600	-1.74164500	-3.90410400
C	0.79936000	-1.69338500	0.34217300
C	0.61271400	-2.96798800	-0.12142700
S	2.07733300	-1.67607100	1.51790500
H	-1.57116200	1.13850300	4.48473900
C	-1.70884400	3.81485200	3.59438900
C	-1.73207200	5.04098500	3.07946000
H	-1.45899100	5.24017600	2.04924100
H	-2.02747900	5.89097200	3.68036300
C	3.36566900	-4.10102500	2.12569800
C	4.21446400	-3.58563200	3.01061600
H	4.22573200	-2.52885700	3.25301200
C	0.92678400	0.87501600	-1.36643700
C	1.51700800	2.46521600	-2.97147400
H	-0.57124600	1.91535800	-2.51889800
H	1.35102300	3.20424300	-3.74445200
C	1.48908400	-3.92166100	0.45487000
H	-0.14076200	-3.21530400	-0.85761600
C	2.35413900	-3.38076200	1.36538800
H	1.48170900	-4.97597300	0.21098100
C	-0.59792000	0.81407900	1.29064900
C	-0.88871600	0.33338400	2.53985100
S	-0.83733800	2.53188400	1.24855900
C	-1.30570900	1.33287700	3.45376200
H	-0.80200700	-0.71334400	2.80015500
C	-1.33445700	2.58680800	2.90737300
H	4.93148900	-4.21275900	3.52383300
C	4.02879500	2.64432500	-3.03913000
C	5.25029500	2.30189000	-2.63943700
H	5.41892300	1.55690600	-1.86989800
H	6.12728400	2.76229800	-3.07502200
C	-5.32049400	-1.82224200	-1.96754400
C	-6.21672300	-1.81499600	-0.98481100
H	-5.96483500	-1.51022500	0.02478800

H	-7.24047700	-2.11620000	-1.16373400	H	3.91808100	3.39753400	-3.81424600
H	3.39945400	-5.16722800	1.91973400	H	-5.62828800	-2.13627700	-2.96104700
H	-1.99211600	3.67276300	4.63359000				

SiVT3

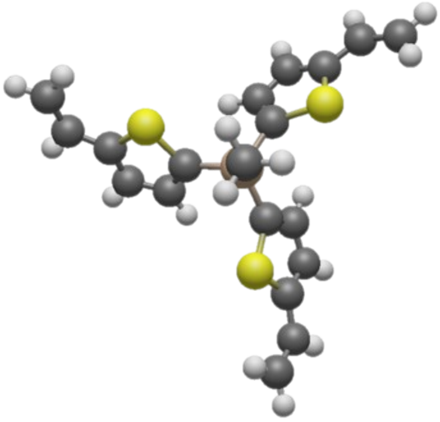

0 1

Si	-0.00012200	0.00018200	0.69063700	C	1.08603500	-6.27917400	0.24331000
C	0.78197600	-1.56188800	0.02762100	C	-0.00030900	0.00024300	2.55896600
C	1.70192500	-1.66387900	-0.98037900	H	-0.53733400	-0.86716400	2.94953700
S	0.40186000	-3.14315700	0.63679100	H	1.01929600	-0.03098100	2.94979300
C	2.09704900	-2.99631800	-1.26511700	H	-0.48316100	0.89898600	2.94942800
H	2.08993500	-0.79983300	-1.50372600	H	0.36531500	-6.01201600	1.00805700
C	1.48203300	-3.92514900	-0.47250500	H	1.30600700	-7.33199100	0.12511400
H	2.81589700	-3.26479700	-2.02824700	H	-5.38990200	2.68885100	1.00858100
C	-1.74392100	0.10396700	0.02742700	H	-7.00330000	2.53442400	0.12546500
C	-2.29214100	-0.64175000	-0.98063400	C	0.96177600	1.45847300	0.02763100
S	-2.92338200	1.22373700	0.63651800	C	0.58963000	2.30725600	-0.97925700
C	-3.64367900	-0.31787100	-1.26534100	S	2.52193000	1.91868500	0.63594700
H	-1.73782500	-1.40970000	-1.50410200	C	1.54615100	3.31558900	-1.26378000
C	-4.14070300	0.67901000	-0.47264000	H	-0.35307300	2.21211100	-1.50200700
H	-4.23556100	-0.80623000	-2.02847700	C	2.65866200	3.24619300	-0.47213100
C	-5.48805900	1.22833000	-0.52088700	H	1.41889000	4.07315600	-2.02607600
H	-6.12605800	0.77171800	-1.27246000	C	3.80848100	4.13782200	-0.52052600
C	1.67985300	-5.36665900	-0.52085100	H	3.73168600	4.91955200	-1.27112200
H	2.39452600	-5.69084800	-1.27220900	C	4.89616600	4.07868300	0.24281400
C	-5.98154100	2.19852000	0.24360500	H	5.69815800	4.79536800	0.12469900

H	5.02538000	3.32020700	1.00679800

SiVT2

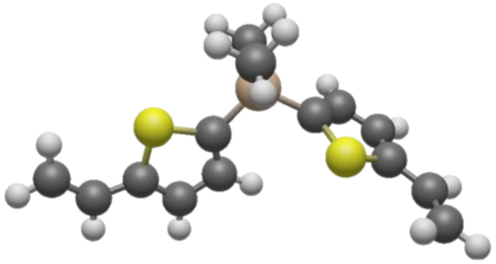

0 1

Si	-0.05029400	1.48905800	0.17433200
C	1.61313000	0.73651600	-0.24068400
C	2.40802900	1.02014100	-1.31841200
S	2.38512400	-0.45987000	0.75235500
C	3.62213900	0.28621500	-1.35042500
H	2.13379400	1.74243100	-2.07629100
C	3.76615400	-0.56633700	-0.29164800
H	4.36879100	0.38326300	-2.12780600
C	-1.35759800	0.18236000	-0.13741600
C	-1.21728900	-1.00292700	-0.80570200
S	-3.00482400	0.36693800	0.38267600
C	-2.41693800	-1.75508300	-0.90391100
H	-0.27160100	-1.33151500	-1.21644100
C	-3.48797500	-1.14955700	-0.30901100
H	-2.48997600	-2.71666900	-1.39522300
C	-4.84511900	-1.67043700	-0.23852300
H	-4.97395400	-2.63660800	-0.71857200
C	4.89658600	-1.44938300	-0.04320600
H	5.67775500	-1.39211900	-0.79617000
C	-5.89449700	-1.09016200	0.33742700
C	5.04707300	-2.28289000	0.98241300
C	-0.10546400	2.01094900	1.97147300
C	-0.33112100	2.96174200	-0.94821000
H	0.07686700	1.16494400	2.63765800
H	0.65053200	2.77216900	2.17804800
H	-1.08212700	2.42908500	2.22881300
H	0.43052200	3.73000500	-0.79475100
H	-0.32047500	2.67063500	-2.00056600
H	-1.30602000	3.41109800	-0.74342200
H	4.29989500	-2.38055000	1.76204000
H	5.93193900	-2.89897600	1.07317600
H	-5.82344300	-0.12710600	0.83048700
H	-6.86584000	-1.56687900	0.33288000

SiVT1

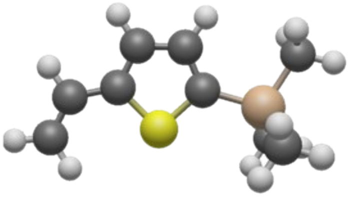

0 1

Si	2.08354800	-0.13677800	-0.00004300
C	0.27416700	0.36994200	0.00007300
C	-0.24367400	1.63648900	-0.00000500
S	-1.02259600	-0.78473100	0.00003600
C	-1.66286000	1.68305400	-0.00006800
H	0.37621000	2.52369000	-0.00000100
C	-2.24522200	0.44700700	-0.00000500
H	-2.23911800	2.59922800	-0.00013500
C	-3.67298600	0.16530600	-0.00001800
H	-4.29965200	1.05295100	-0.00022500
C	-4.25078400	-1.03300000	0.00019200
C	2.44572300	-1.15556100	-1.53367300
H	2.23542500	-0.58822400	-2.44320200
H	3.49529900	-1.46078100	-1.56200700
H	1.83675100	-2.06256600	-1.56188300
H	-3.67490800	-1.95167400	0.00045700
H	-5.32837500	-1.13104400	0.00010800
C	2.44602500	-1.15655500	1.53286300
C	3.11189100	1.43201300	0.00066600
H	3.49568400	-1.46157800	1.56066300
H	2.23593100	-0.58983700	2.44282100
H	1.83727600	-2.06371600	1.56069600
H	2.91545300	2.04325900	-0.88328800
H	2.91510800	2.04242300	0.88512600
H	4.17709800	1.18628100	0.00075700

GeVT4

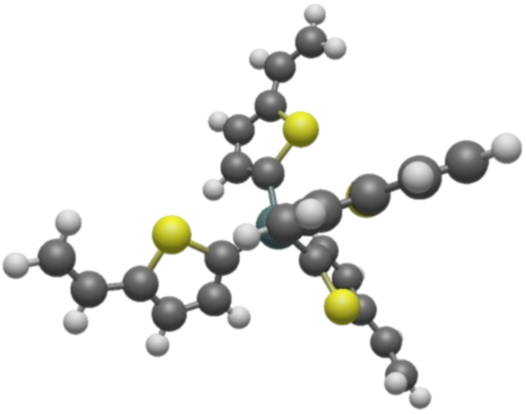

0 1

Ge	-0.21090100	-0.10950600	-0.13286900	C	0.01311400	-0.01206400	2.82801000
C	0.96301200	-1.17384700	-1.25039900	S	2.23214800	0.71599800	1.80063500
C	1.26355300	-0.93805700	-2.56197200	C	0.86959200	0.29370900	3.91753700
S	1.77045900	-2.60367900	-0.69615200	H	-1.00450700	-0.35876300	2.94840100
C	2.13626900	-1.90520800	-3.12541800	C	2.11335200	0.70871700	3.53154400
H	0.87309000	-0.08980400	-3.10884800	H	0.57951500	0.20779400	4.95657100
C	2.50537600	-2.88262000	-2.24384100	C	3.20859700	1.08738200	4.41257300
H	2.48683500	-1.88021800	-4.14897200	H	2.96871200	1.02269100	5.47025300
C	-1.89707300	-1.04340000	0.08216000	C	3.39067700	-4.00455400	-2.52133200
C	-2.17283000	-2.32030800	-0.31714800	H	3.76289500	-4.03320700	-3.54166000
S	-3.28987000	-0.33765500	0.83704600	C	-5.62132300	-1.89965700	1.04890400
C	-3.49656600	-2.73572500	-0.01535000	H	-6.06843400	-2.86601300	0.83295600
H	-1.44807700	-2.94894400	-0.81726500	C	-0.17493100	5.23510200	-2.43230700
C	-4.23692100	-1.77616100	0.61578300	H	-0.88373600	5.66540200	-3.13436300
H	-3.89300200	-3.71300000	-0.25802100	C	4.42336100	1.48796700	4.04788200
C	-0.55214200	1.56674700	-1.04805000	C	0.85497600	5.96926800	-2.02073600
C	-1.59089500	1.82394900	-1.89849300	C	-6.35159600	-0.97065100	1.65950500
S	0.48639300	2.94782800	-0.93397500	C	3.76587600	-4.95412500	-1.66884300
C	-1.55297000	3.12640200	-2.46079800	H	3.42681700	-4.97332000	-0.63910500
H	-2.36855800	1.10262300	-2.11290600	H	4.43240300	-5.74807300	-1.97893900
C	-0.48349900	3.86723100	-2.04047800	H	0.99278700	6.98215500	-2.37549100
H	-2.29371100	3.50950600	-3.15052200	H	1.59127300	5.59099500	-1.32042600
C	0.59925600	0.16862900	1.60700200	H	4.71648900	1.57057900	3.00725500

H	5.16887200	1.74738400	4.78794600
H	-5.95654200	0.01033200	1.89897300
H	-7.37797100	-1.16615500	1.94070400

SnVT4

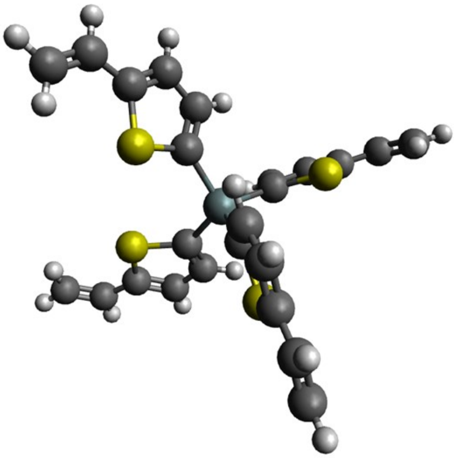

0 1

Sn	0.07369200	0.10430600	-0.16033300
C	-1.04882700	-1.11859400	-1.45182900
C	-0.55172700	-1.97701000	-2.40954500
S	-2.84572100	-1.21669600	-1.41927100
C	-1.55310100	-2.71928600	-3.12417800
H	0.50852600	-2.08738200	-2.60929600
C	-2.84155200	-2.44462800	-2.72903500
H	-1.32135300	-3.43406800	-3.90544900
C	1.74307300	0.71777200	-1.28588800
C	1.79924900	0.89919700	-2.65172600
S	3.33696700	1.12183600	-0.55185300
C	3.07063600	1.35465200	-3.14292300
H	0.95334100	0.71275300	-3.30419500
C	4.01857500	1.53146900	-2.16182700
H	3.27275700	1.54210200	-4.19128000
C	0.97841100	1.82154700	0.44316600
C	0.71949100	3.11454200	0.04259100
S	-2.38502000	1.80207300	1.56794200
C	-1.60454600	4.10145100	0.59812000
H	0.08834800	3.36762400	-0.63516300
C	-2.56339500	3.58521300	1.43770800
H	-1.52875400	5.16040100	0.37944100
C	0.64944300	-0.91701600	1.58264500
C	0.69067500	-0.40365400	2.86106100
S	1.19727300	-2.63153100	1.59485200
C	1.14856500	-1.32847700	3.86080200
H	0.39537900	0.61271200	3.09678000
C	1.46855000	-2.57230700	3.36880100
H	1.23473000	-1.07599200	4.91139400
C	-4.05967100	-3.03855800	-3.27085200
H	-3.88802400	-3.76804200	-4.06201600
C	5.39380100	1.97992700	-2.35682500
H	5.65367500	2.18852300	-3.39436800
C	-3.59483200	4.33815400	2.14422100
H	-3.56585900	5.41268300	1.96527000
C	1.95585000	-3.71057300	4.14128200
H	2.06549100	-3.51324000	5.20739200
C	-5.32411400	-2.77290800	-2.89090400
C	2.26811700	-4.93216700	3.66801800
C	-4.53968100	3.83774300	2.96316700
C	6.32901700	2.14990700	-1.40276900
H	7.32881100	2.48897200	-1.65350500

H	6.12718000	1.95588300	-0.35208000
H	-6.16574700	-3.27239100	-3.35953000
H	-5.55522100	-2.05569100	-2.10699800
H	2.62409600	-5.71466200	4.33015300
H	2.17784100	-5.18576200	2.61452900
H	-5.26532900	4.48660400	3.44255900
H	-4.61768000	2.77439100	3.1766170

SiVT4 dimer

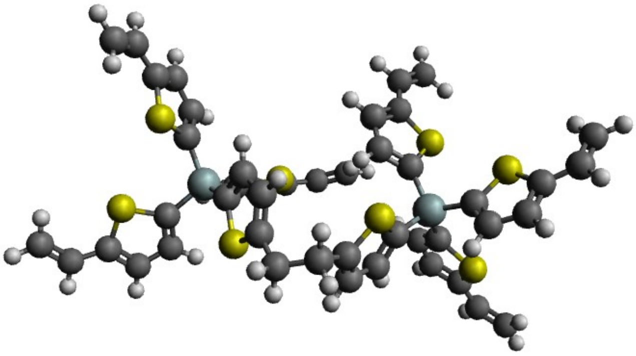

0 1

Si	4.34108200	0.03599100	-0.36096600
C	5.64073900	1.33553900	-0.69441600
C	5.48010000	2.50872800	-1.38338900
S	7.25182800	1.24364100	-0.05809700
C	6.63694300	3.32759200	-1.39772700
H	4.55371500	2.77884000	-1.87328800
C	7.69256800	2.78337200	-0.71907500
H	6.69430100	4.28675700	-1.89573900
C	3.28640400	-0.07920500	-1.89511700
C	3.68115100	0.08286300	-3.19693400
S	1.60598600	-0.50949400	-1.83739600
C	2.64661700	-0.13829200	-4.13989400
H	4.69057600	0.35952500	-3.47193200
C	1.45191600	-0.47484300	-3.56350700
H	2.77389600	-0.05099500	-5.21114400
C	5.11186900	-1.63260300	-0.03819200
C	5.16095300	-2.68399500	-0.91364000
S	5.93683100	-2.05270500	1.43139500
C	5.85682700	-3.81410000	-0.41491400
H	4.70445900	-2.64634700	-1.89398700
C	6.34639000	-3.63372200	0.84898200
H	5.99147400	-4.73480500	-0.96750400
C	3.31552000	0.50847400	1.11904300
C	2.74286900	-0.31764000	2.04924800
S	2.87336000	2.15016000	1.46197100
C	1.95959200	0.35975300	3.02148400
H	2.88051100	-1.39098100	2.04224100
C	1.92908800	1.71018700	2.83733700
H	1.44153900	-0.14569500	3.82576600
C	1.23965900	2.76123300	3.66015000
H	1.81724300	2.94746600	4.57101100
H	1.23097400	3.70568900	3.11126900
C	-0.19589400	2.39353700	4.06207000
H	-0.59271300	3.19276200	4.69550200
H	-0.18114400	1.49626000	4.68489300
C	-1.11310200	2.17892600	2.89209800
C	-1.29968100	2.96514400	1.79531500
S	-2.12646400	0.78283800	2.80892000
C	-2.25366900	2.43628000	0.88475100
H	-0.77006700	3.89408000	1.62976200
C	-2.80399400	1.24682800	1.27926000

H	-2.52482700	2.92160400	-0.04378500
Si	-4.03799600	0.22888700	0.32835400
C	-4.60492800	1.20490000	-1.15620300
C	-3.99262800	1.30400400	-2.37739100
S	-6.01134900	2.21999100	-1.11573400
C	-4.64375700	2.18941400	-3.27204000
H	-3.09583800	0.75377900	-2.63194100
C	-5.76089600	2.77272400	-2.73840100
H	-4.30502600	2.38915700	-4.28036500
C	-3.22914900	-1.34621200	-0.26724100
C	-2.01454000	-1.85079200	0.11435900
S	-3.99062400	-2.43404600	-1.38773000
C	-1.70048700	-3.10052400	-0.47855400
H	-1.35550100	-1.33687300	0.80104300
C	-2.67522400	-3.56174800	-1.31902200
H	-0.78090800	-3.64127400	-0.29690300
C	-5.49254500	-0.12754500	1.44285900
C	-5.90133200	0.63026400	2.50825900
S	-6.59229900	-1.44815100	1.20468800
C	-7.08723800	0.15920000	3.12521500
H	-5.36123100	1.50567900	2.84399300
C	-7.59348700	-0.96548800	2.53425400
H	-7.55273300	0.62937700	3.98162600
C	-8.78947500	-1.68835900	2.94288600
H	-9.30094800	-1.25236700	3.79656600
C	-2.64349400	-4.80464500	-2.07644900
H	-1.72899300	-5.37736600	-1.95052100
C	-6.64153400	3.71699400	-3.41163100
H	-6.34079100	3.95664600	-4.42781300
C	9.01328600	3.37633800	-0.56342600
H	9.12254500	4.34659900	-1.04001500
C	0.21080200	-0.76096800	-4.27026300
H	0.28275700	-0.65458600	-5.34926600
C	7.09737500	-4.60705500	1.62906600
H	7.25870700	-5.55344700	1.12042500
C	-9.28626200	-2.78829100	2.38380800
C	-3.59926600	-5.27662400	-2.87202500
C	7.58177800	-4.44151800	2.85674200
C	-0.94699300	-1.13359900	-3.73155800
C	10.05073400	2.85346600	0.08430800
H	9.99769300	1.88933900	0.57753700
H	10.99409700	3.38047600	0.14060800
H	-1.80984900	-1.33213700	-4.35388500
H	-1.07481400	-1.26875700	-2.66336200
H	8.12940100	-5.23374200	3.34999600
H	7.45185600	-3.51777500	3.40943800
H	-3.47498200	-6.21674800	-3.39312900
H	-4.53293400	-4.74832100	-3.02987600
H	-10.18689600	-3.24908200	2.76771900
H	-8.81687700	-3.26527400	1.53072500
C	-7.73449100	4.28526000	-2.90978800
H	-8.08105300	4.08154100	-1.90280500
H	-8.32180000	4.97743200	-3.49871400

S8. References

1 A. B. Pangborn, M. A. Giardello, R. H. Grubbs, R. K. Rosen and F. J. Timmers, *Organometallics*, 1996, **15**, 1518-1520.

2 Y. Kurishiba, A. Oguri, D. Yamamoto, C. Homma, R. Goseki and T. Ishizone, *Macromolecules*, 2024, **57**, 8601–8609.

3 Tsyurupa, M. P.; Borisov, Y. A.; Blinnikova, Z. K.; Platonova, N. P.; Ul’yanov, A. V.; Buryak, A. K.; Davankov, V. A. On the Origin of Absorbance Band around 1700 Cm−1 in FTIR Spectra of Hypercrosslinked Polystyrene. Prot. Met. Phys. Chem. Surf. 2014, 50 (1), 59–63.

4 Tsyurupa, M. P.; Blinnikova, Z. K.; Davidovich, Y. A.; Lyubimov, S. E.; Naumkin, A. V.; Davankov, V. A. On the Nature of “Functional Groups” in Non-Functionalized Hypercrosslinked Polystyrenes. React. Funct. Polym. 2012, 72 (12), 973–982.

5 M. J. Frisch, G. W. Trucks, H. B. Schlegel, G. E. Scuseria, M. A. Robb, J. R. Cheeseman, G. Scalmani, V. Barone, G. A. Petersson, H. Nakatsuji, X. Li, M. Caricato, A. V. Marenich, J. Bloino, B. G. Janesko, R. Gomperts, B. Mennucci, H. P. Hratchian, J. V. Ortiz, A. F. Izmaylov, J. L. Sonnenberg, D. Williams-Young, F. Ding, F. Lipparini, F. Egidi, J. Goings, B. Peng, A. Petrone, T. Henderson, D. Ranasinghe, V. G. Zakrzewski, J. Gao, N. Rega, G. Zheng, W. Liang, M. Hada, M. Ehara, K. Toyota, R. Fukuda, J. Hasegawa, M. Ishida, T. Nakajima, Y. Honda, O. Kitao, H. Nakai, T. Vreven, K. Throssell, J. A. Montgomery, Jr., J. E. Peralta, F. Ogliaro, M. J. Bearpark, J. J. Heyd, E. N. Brothers, K. N. Kudin, V. N. Staroverov, T. A. Keith, R. Kobayashi, J. Normand, K. Raghavachari, A. P. Rendell, J. C. Burant, S. S. Iyengar, J. Tomasi, M. Cossi, J. M. Millam, M. Klene, C. Adamo, R. Cammi, J. W. Ochterski, R. L. Martin, K. Morokuma, O. Farkas, J. B. Foresman, and D. J. Fox, Gaussian, Inc., Wallingford CT, 2016.

6 T. Yanai, D. P. Tew and N. C. Handy, *Chem. Phys. Lett.*, 2004, **393**, 51–57.